Gamma-ray strength functions in ^{74}Ge

Ronald Schwengner

Institute of Radiation Physics, Helmholtz-Zentrum Dresden-Rossendorf
01328 Dresden, Germany

- Dipole strength up to the neutron-separation energy:
  - Photon-scattering experiments at γELBE

- M1 and E2 strength at low energy:
  - Shell-model calculations

HZDR

HELMHOLTZ ZENTRUM DRESDEN ROSSENDORF

Study of germanium isotopes

- Extraction of neutron-capture cross sections for astrophysically relevant neutron energies.
- Test of strength functions deduced from different reactions.
- Combination of experiments using neutron capture and alternative reaction techniques in an international collaboration:
  - Neutron capture at IKI Budapest.
  - Discrete γ-ray spectroscopy at STARS-LIBERACE (LBNL) and AFRODITE (iThemba).
  - Statistical γ-ray measurements at CACTUS (Oslo) and γELBE (HZDR).

The bremsstrahlung facility at the electron accelerator ELBE

Accelerator parameters:

- Maximum electron energy:
  $\approx$ 18 MeV
- Maximum average current:
  $\approx$ 0.8 mA
- Micro-pulse rate:
  13 MHz
- Micro-pulse length:
  $\approx$ 5 ps

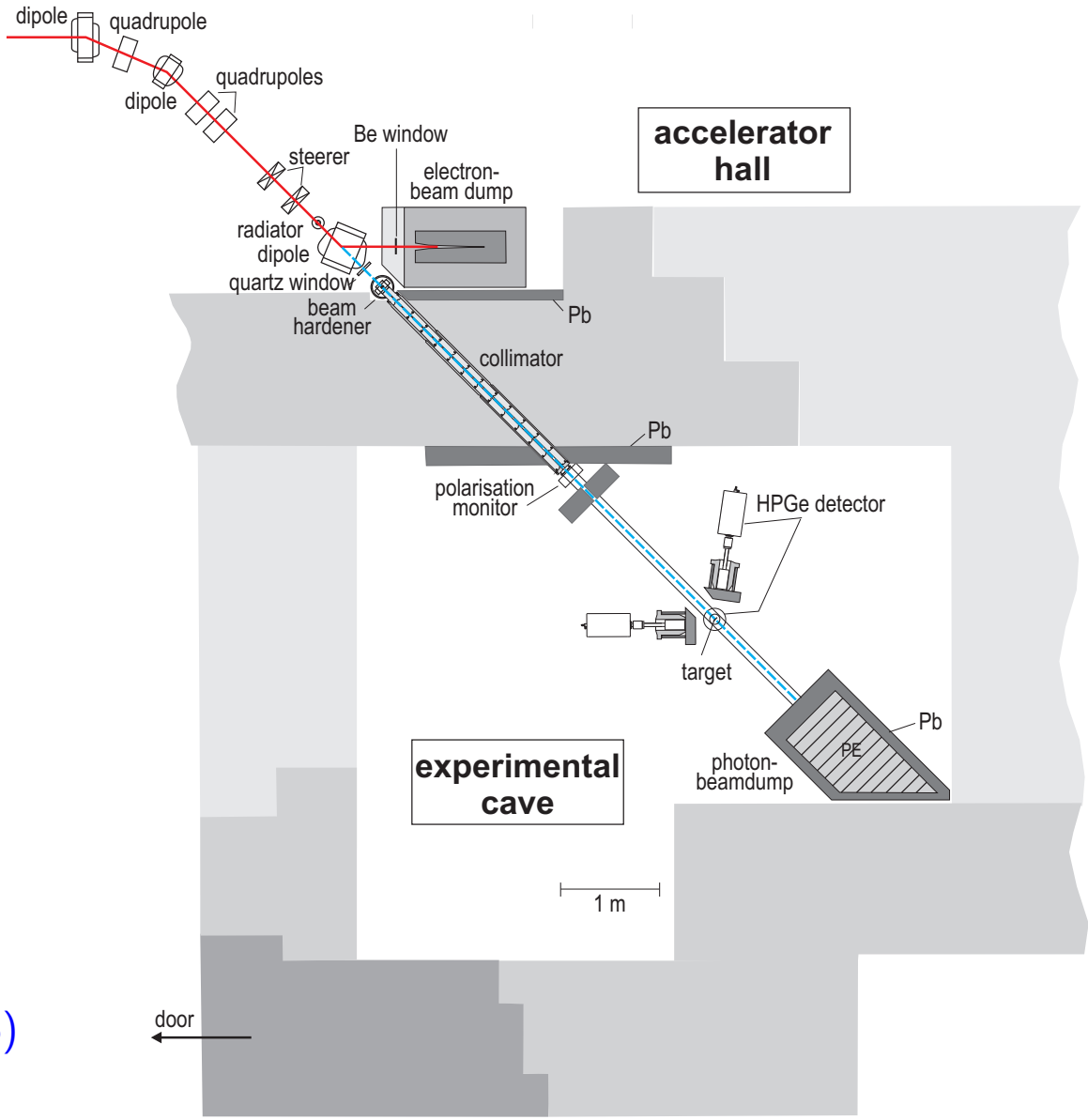

R.S. et al., NIM A 555, 211 (2005)

Detector setup at γELBE

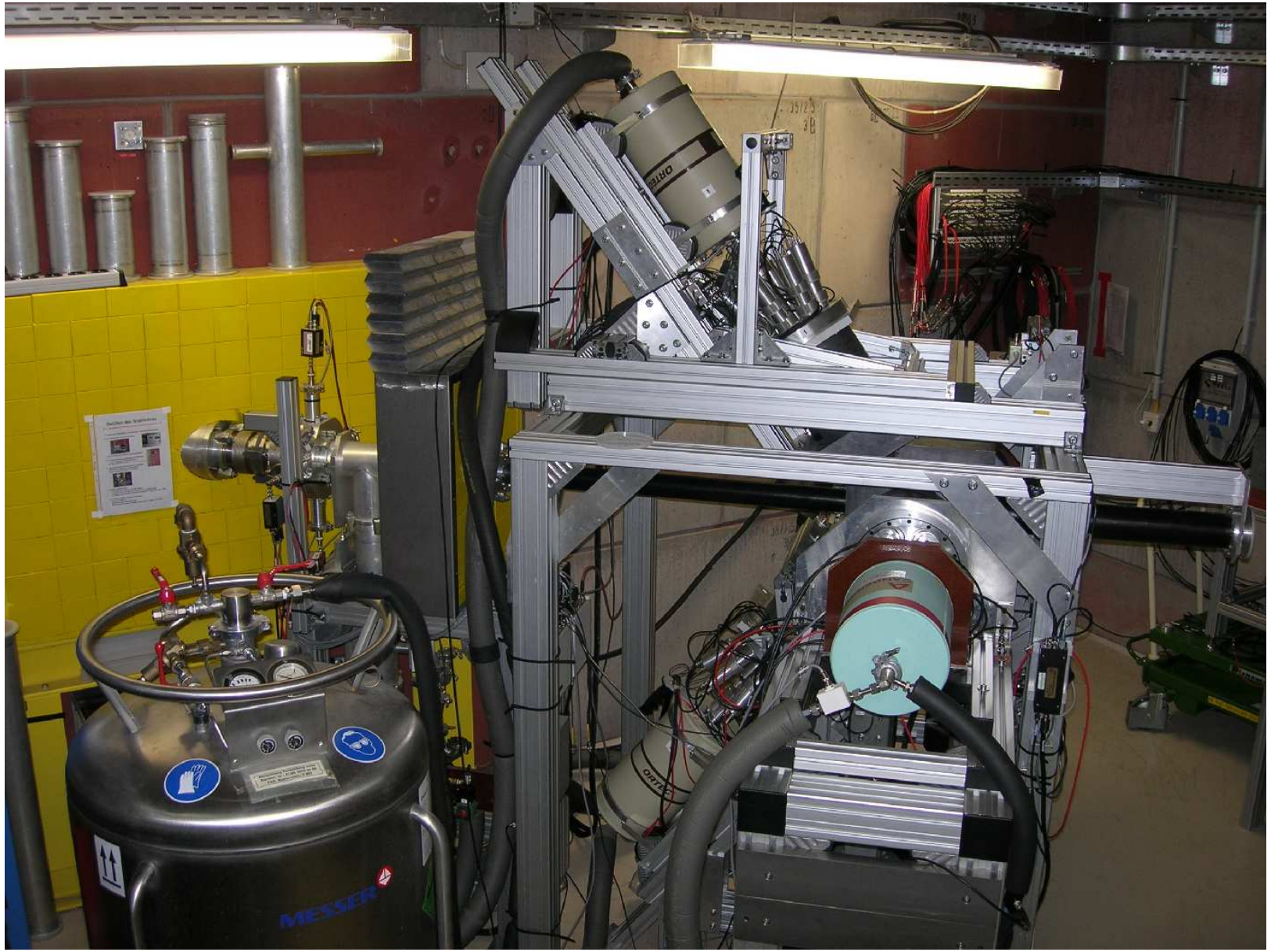

Measurement at γELBE

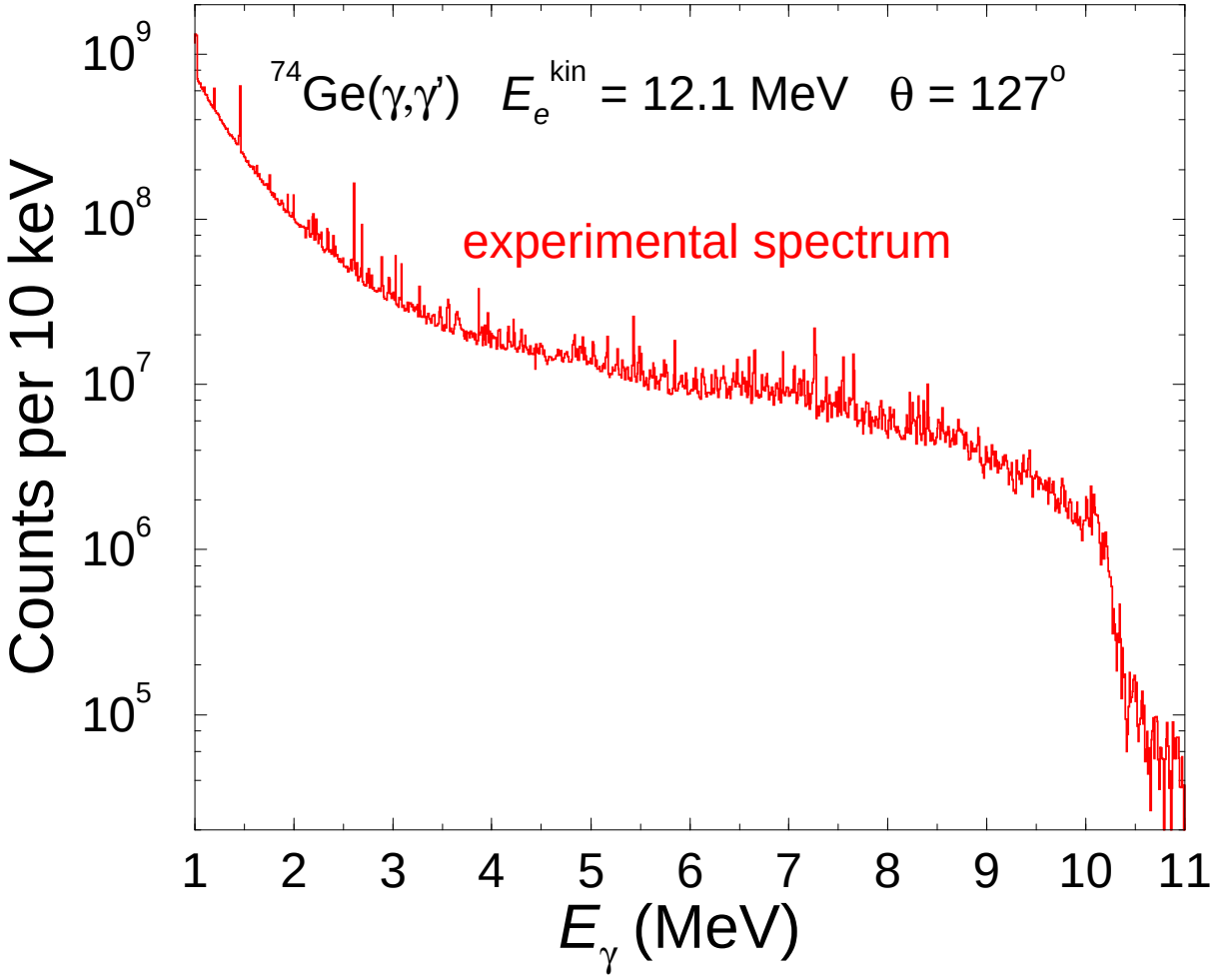

Measurement at γELBE

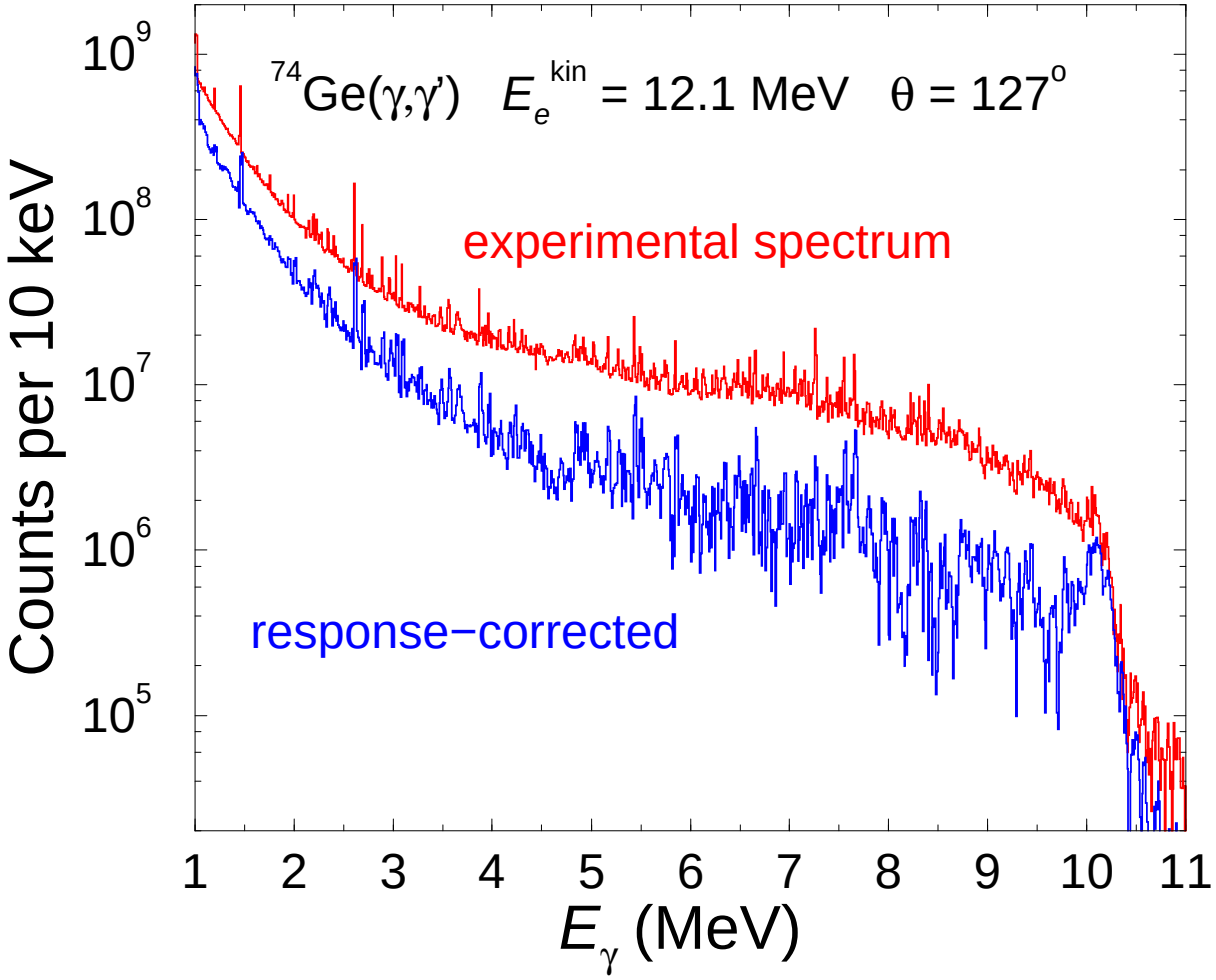

Measurement at γELBE

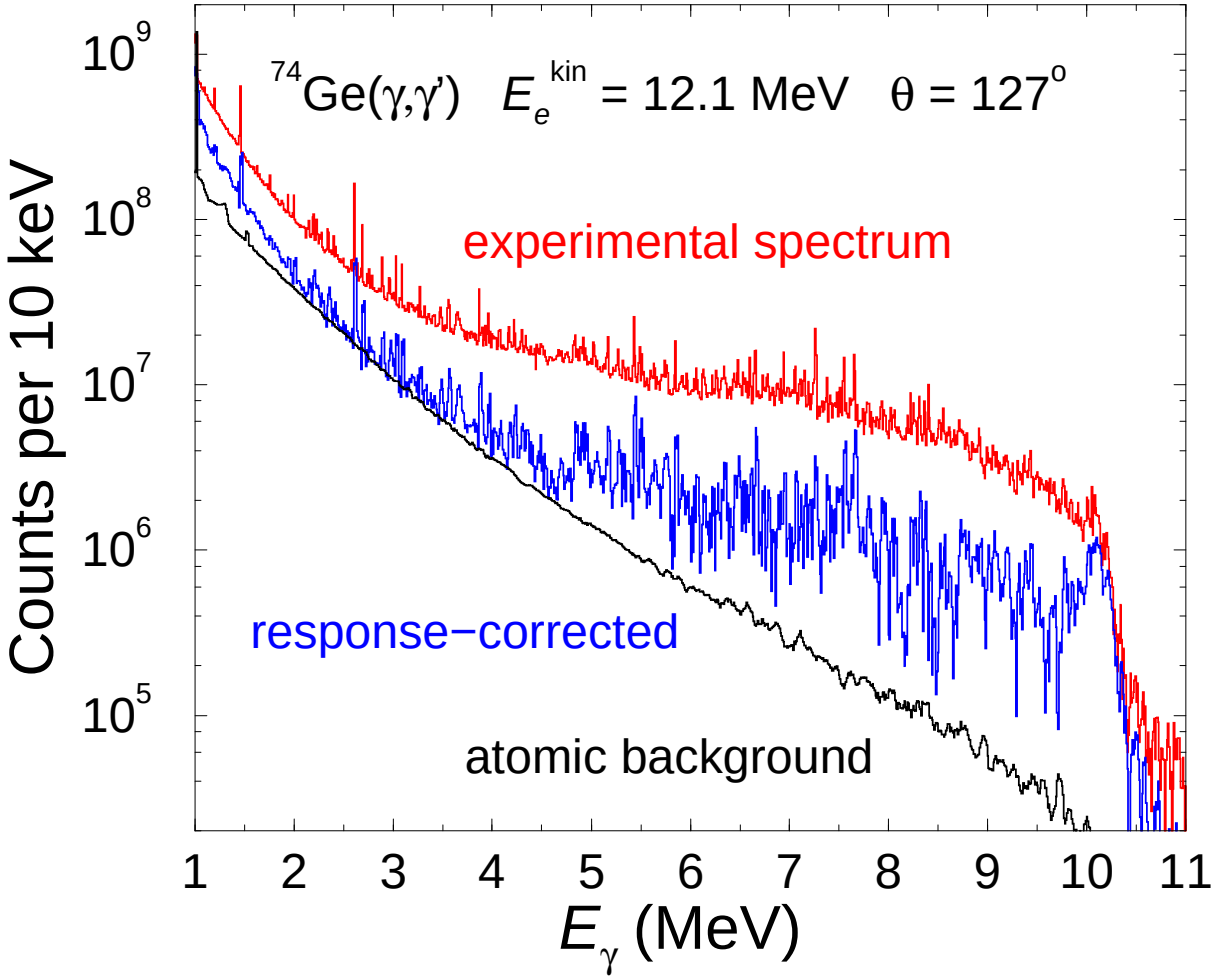

Photon scattering - feeding and branching

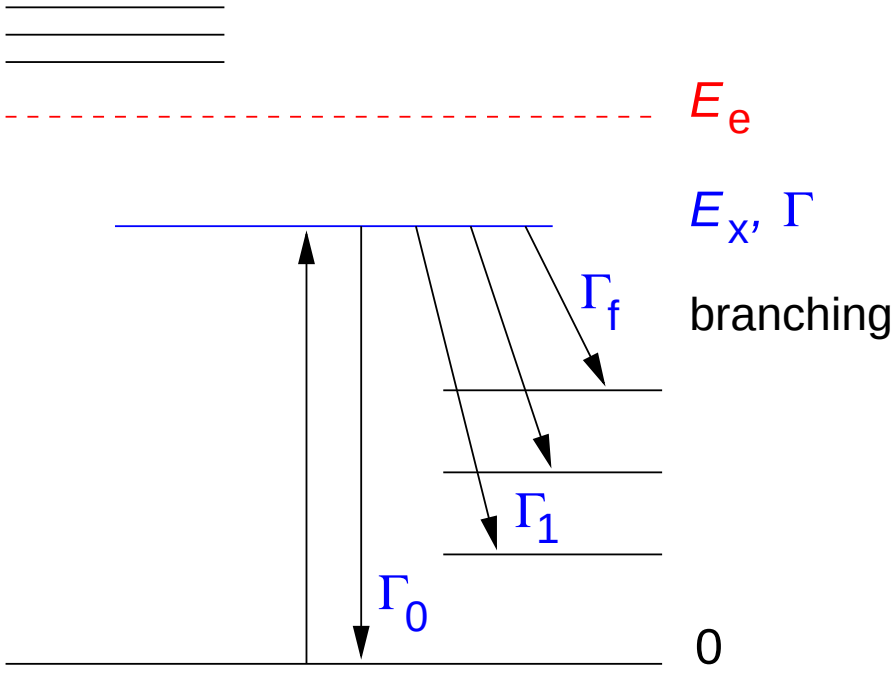

Measured intensity of a γ transition:

$$I_\gamma(E_\gamma, \Theta) = I_s(E_x)\, \Phi_\gamma(E_x)\, \epsilon(E_\gamma)\, N_{at}\, W(\Theta)\, \Delta\Omega$$

Integrated scattering cross section:

$$I_s = \int \sigma_{\gamma\gamma}\, dE = \frac{2J_x + 1}{2J_0 + 1} \left(\frac{\pi\hbar c}{E_x}\right)^2 \frac{\Gamma_0}{\Gamma}\, \Gamma_0$$

Absorption cross section:

$$\sigma_\gamma = \sigma_{\gamma\gamma} \left(\frac{\Gamma_0}{\Gamma}\right)^{-1}$$

E1 strength:

$$B(E1) \sim \Gamma_0 / E_\gamma^3$$

Photon scattering - feeding and branching

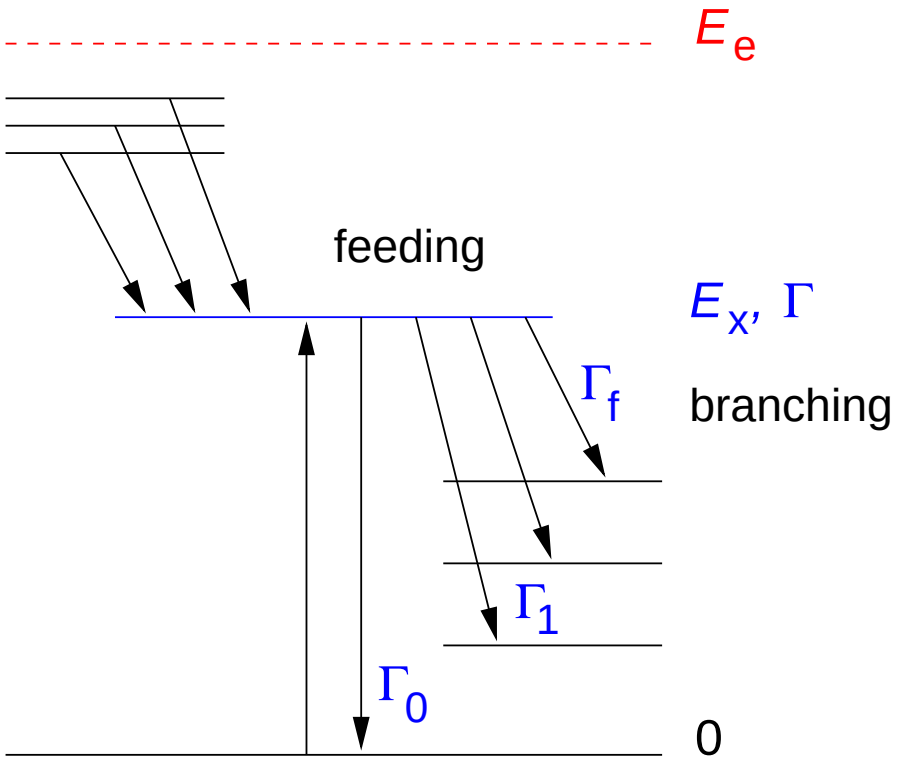

Measured intensity of a γ transition:

$$I_\gamma(E_\gamma, \Theta) > I_s(E_x)\, \Phi_\gamma(E_x)\, \epsilon(E_\gamma)\, N_{at}\, W(\Theta)\, \Delta\Omega$$

Integrated scattering cross section:

$$I_s = \int \sigma_{\gamma\gamma}\, dE = \frac{2J_x + 1}{2J_0 + 1} \left(\frac{\pi\hbar c}{E_x}\right)^2 \frac{\Gamma_0}{\Gamma}\, \Gamma_0$$

Absorption cross section:

$$\sigma_\gamma = \sigma_{\gamma\gamma} \left(\frac{\Gamma_0}{\Gamma}\right)^{-1}$$

E1 strength:

$$B(E1) \sim \Gamma_0 / E_\gamma^3$$

Simulations of γ-ray cascades

Code γDEX:
G. Schramm et al., PRC 85, 014311 (2012)
R. Massarczyk et al., PRC 86, 014319 (2012); PRC 87, 044306 (2013)

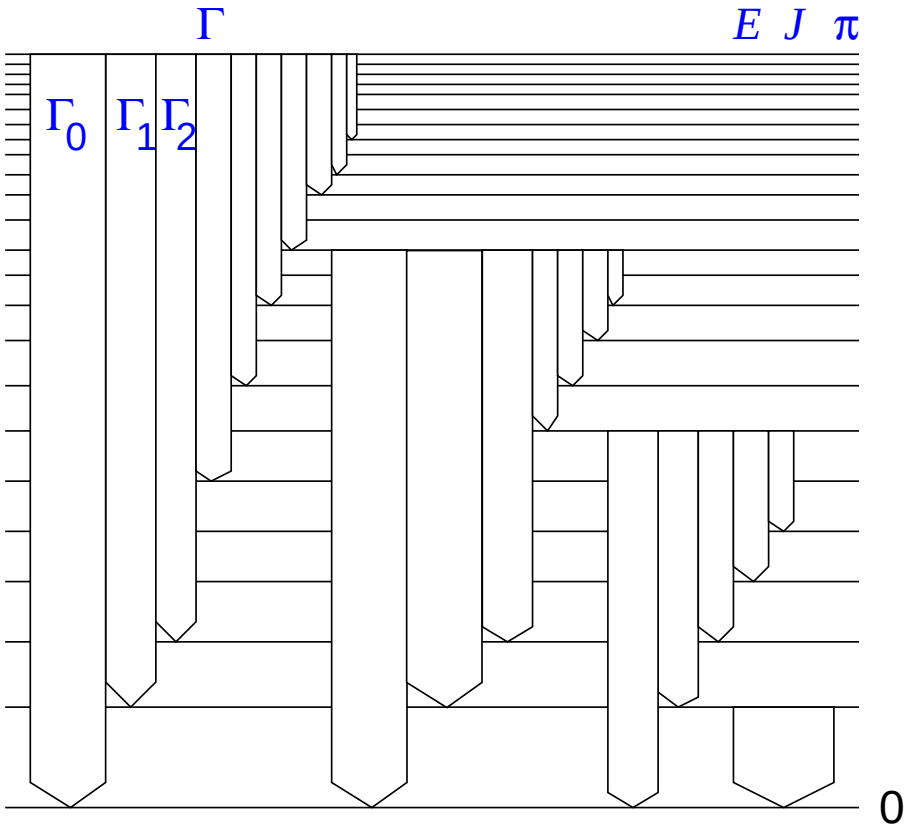

⇒ Level scheme of $J = |J_0 \pm 1, ..., 5|$ states in 10 keV energy bins constructed by using:
- Constant-Temperature Model with level-density parameters from T. v. Egidy, D. Bucurescu, PRC 80, 054310 (2009).
- Parity distribution of level densities according to S. I. Al-Quraishi et al., PRC 67, 015803 (2003).
- Wigner level-spacing distributions.

⇒ Partial decay widths calculated by using:
- Photon strength functions approximated by Lorentz curves (www-nds.iaea.org/RIPL-2).
- Porter-Thomas distributions of decay widths.

⇒ Subtraction of feeding intensities and correction of intensities of g.s. transitions with calculated branching ratios Γ_0/Γ.

⇒ Determination of the absorption cross section.

Average branching ratios of ground-state transitions in ^{74}Ge

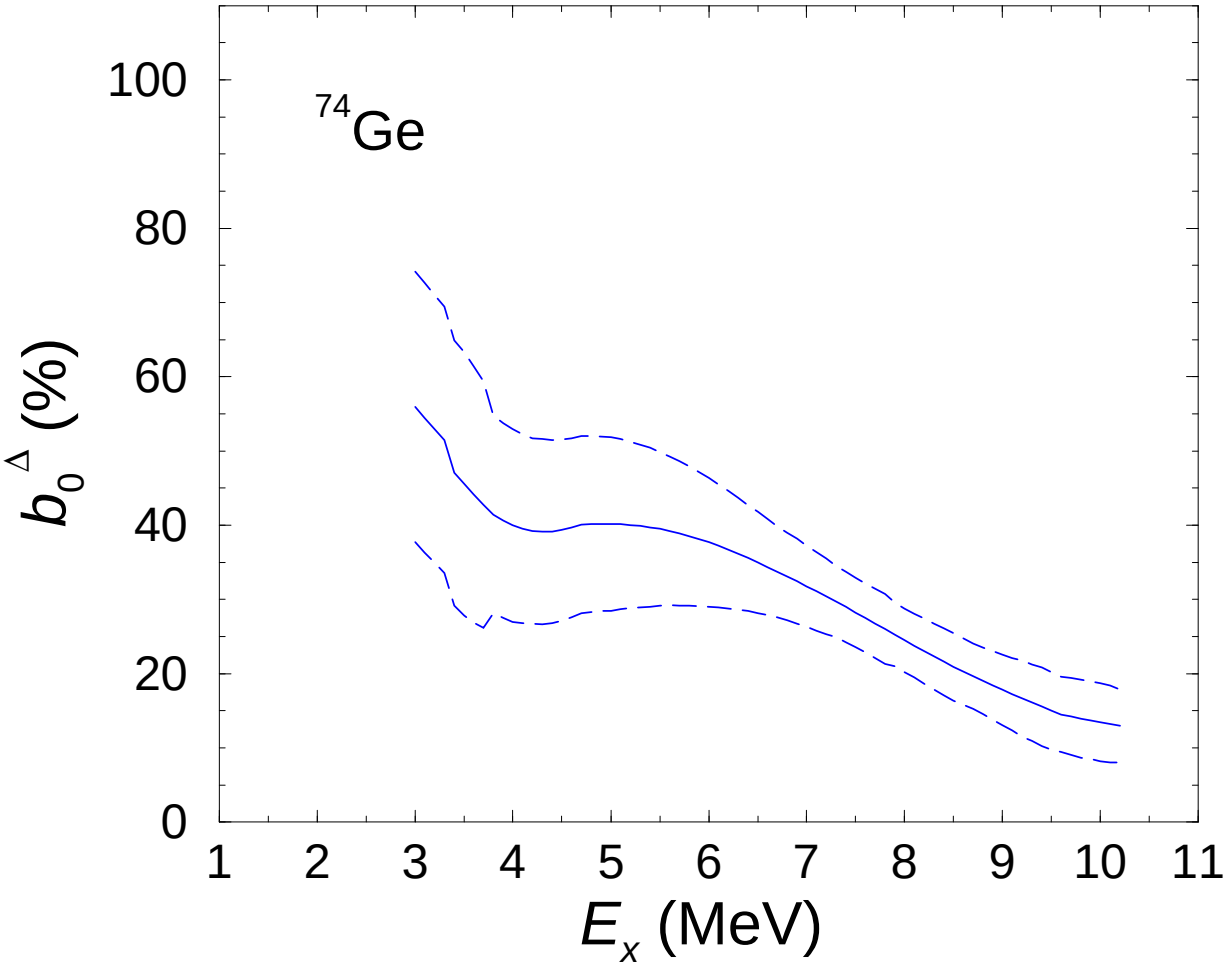

Iterative determination of the absorption cross section

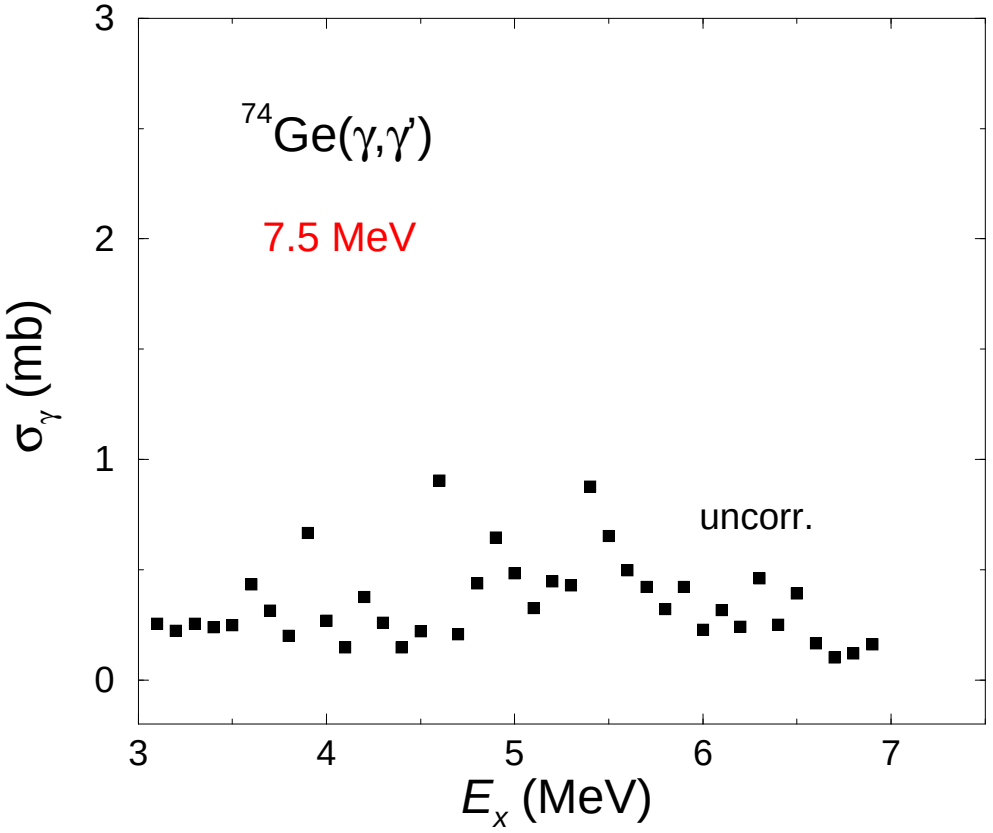

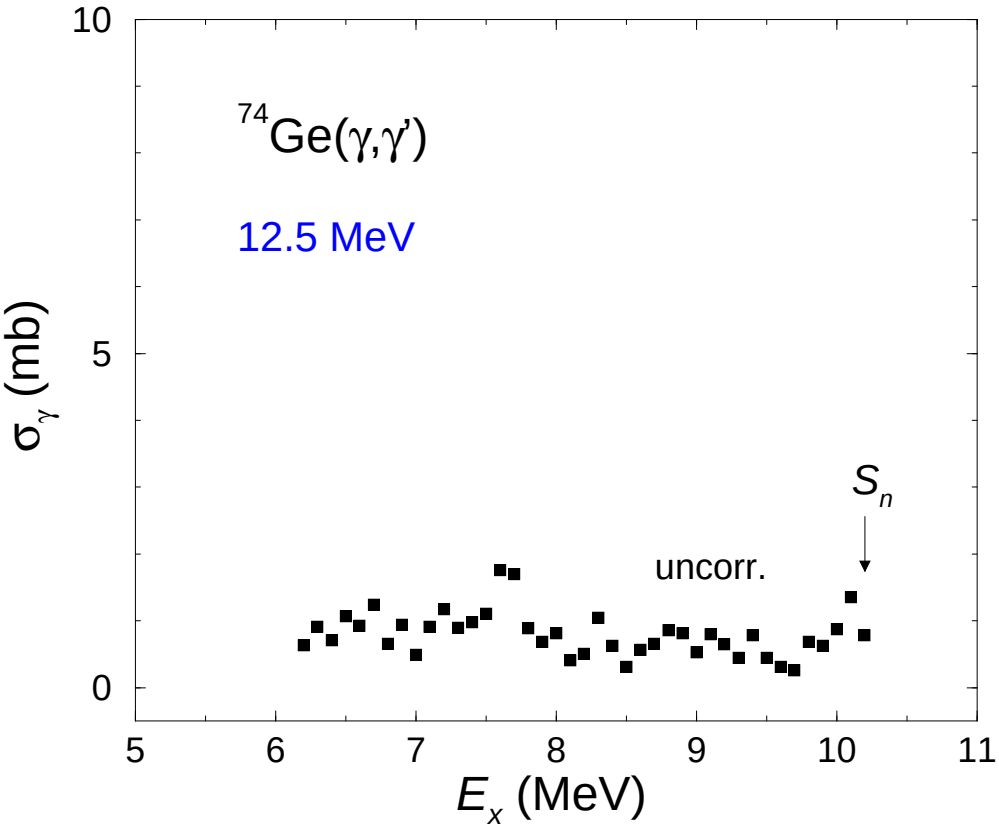

Cross section including strength of resolved peaks and of quasi-continuum.

Iterative determination of the absorption cross section

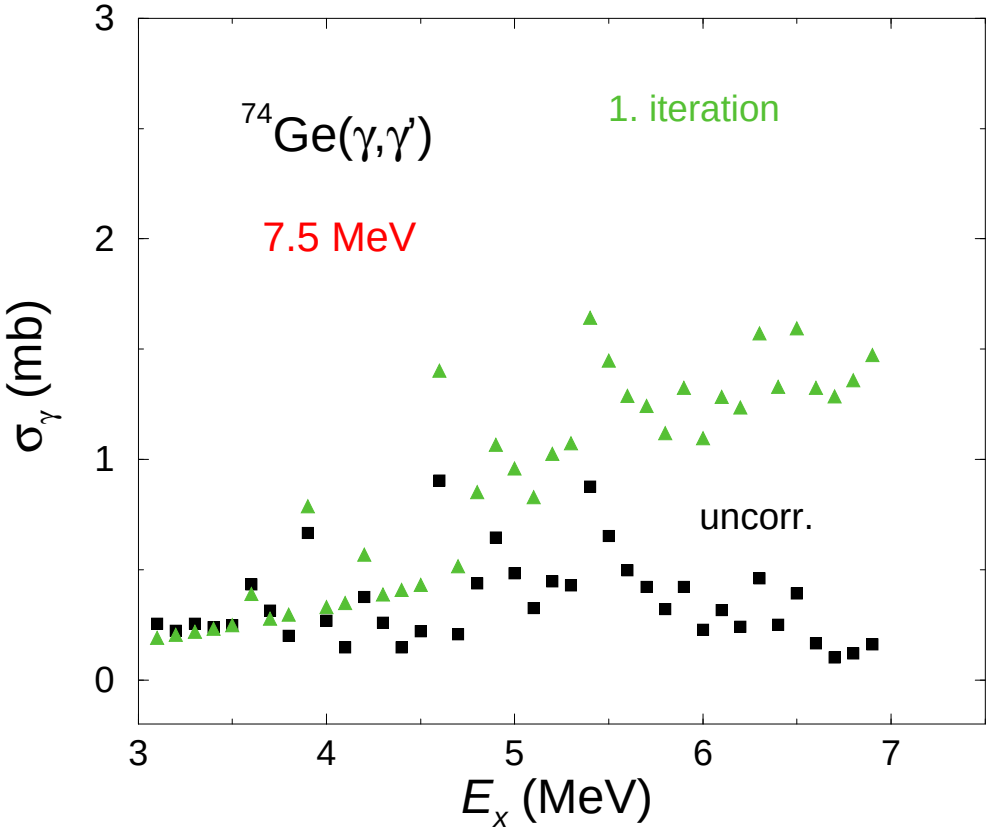

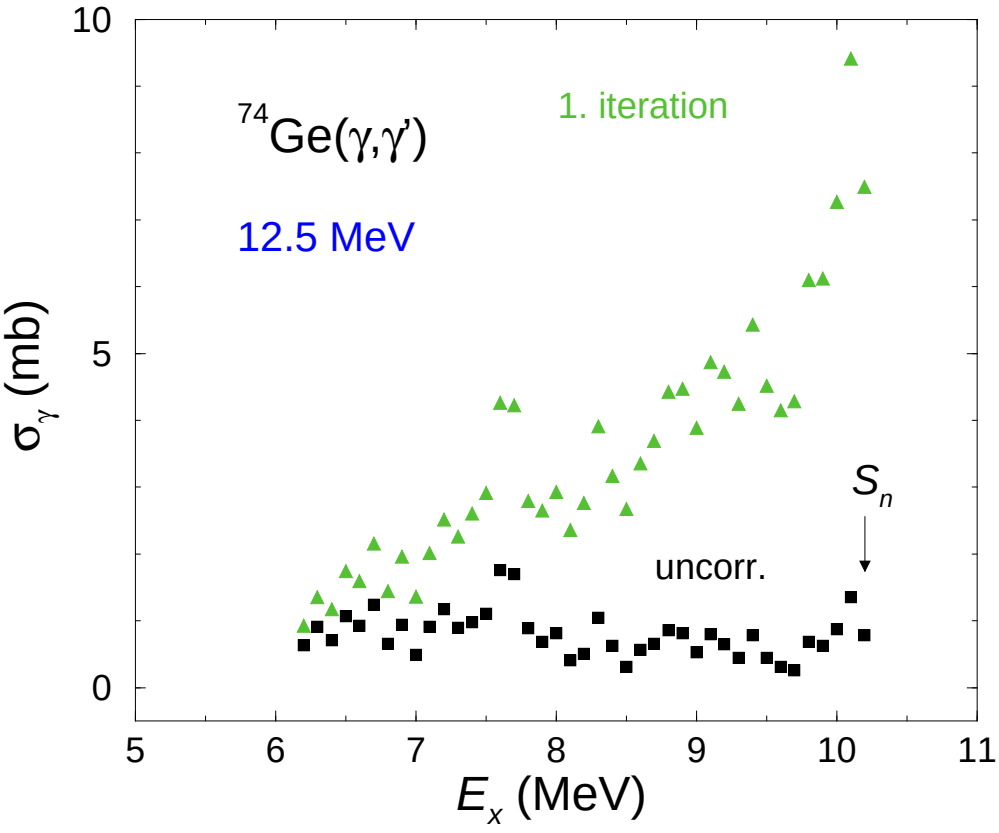

Cross section including strength of resolved peaks and of quasi-continuum.

Result of the correction for feeding intensities and branching ratios used as input for the next calculation.

Iterative determination of the absorption cross section

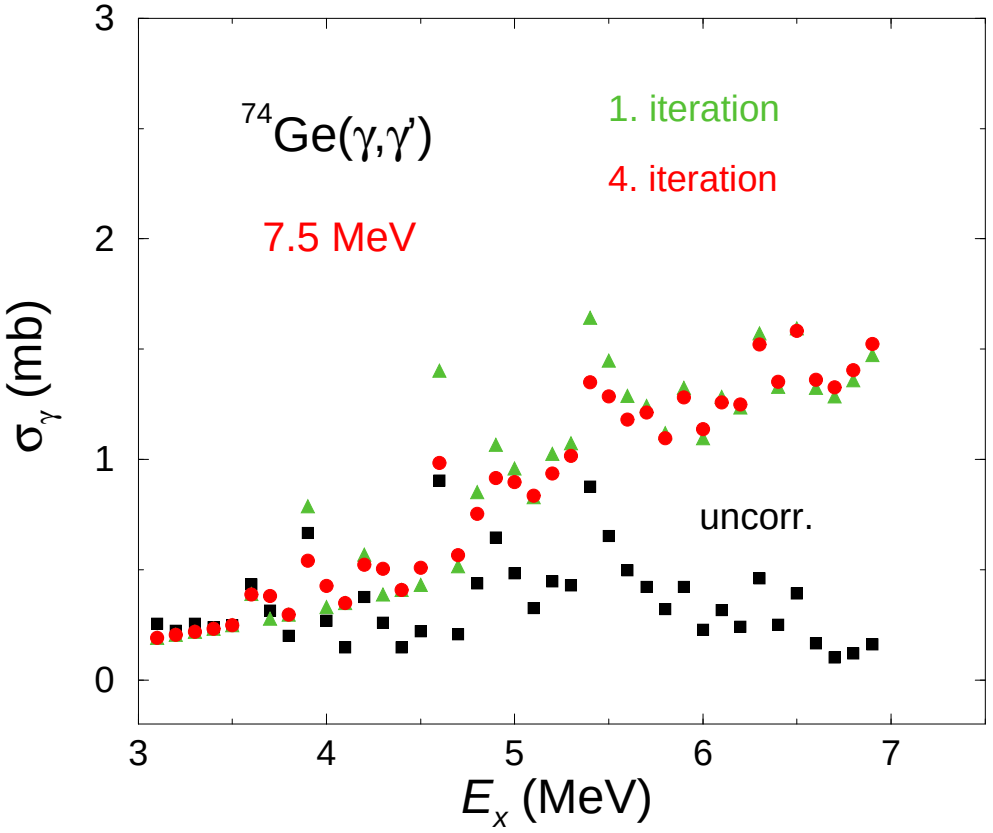

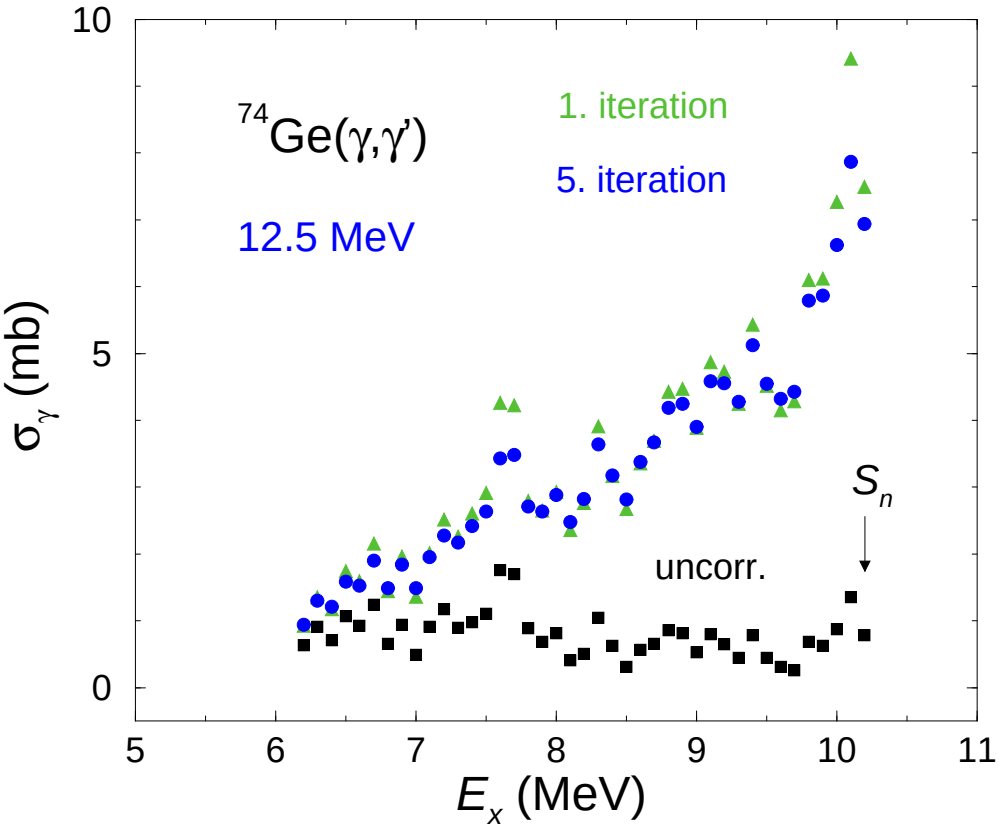

Cross section including strength of resolved peaks and of quasi-continuum.

Result of the correction for feeding intensities and branching ratios → used as input for the next calculation.

Convergence criteria fulfilled → data taken as final results.

Absorption cross section of ^{74}Ge

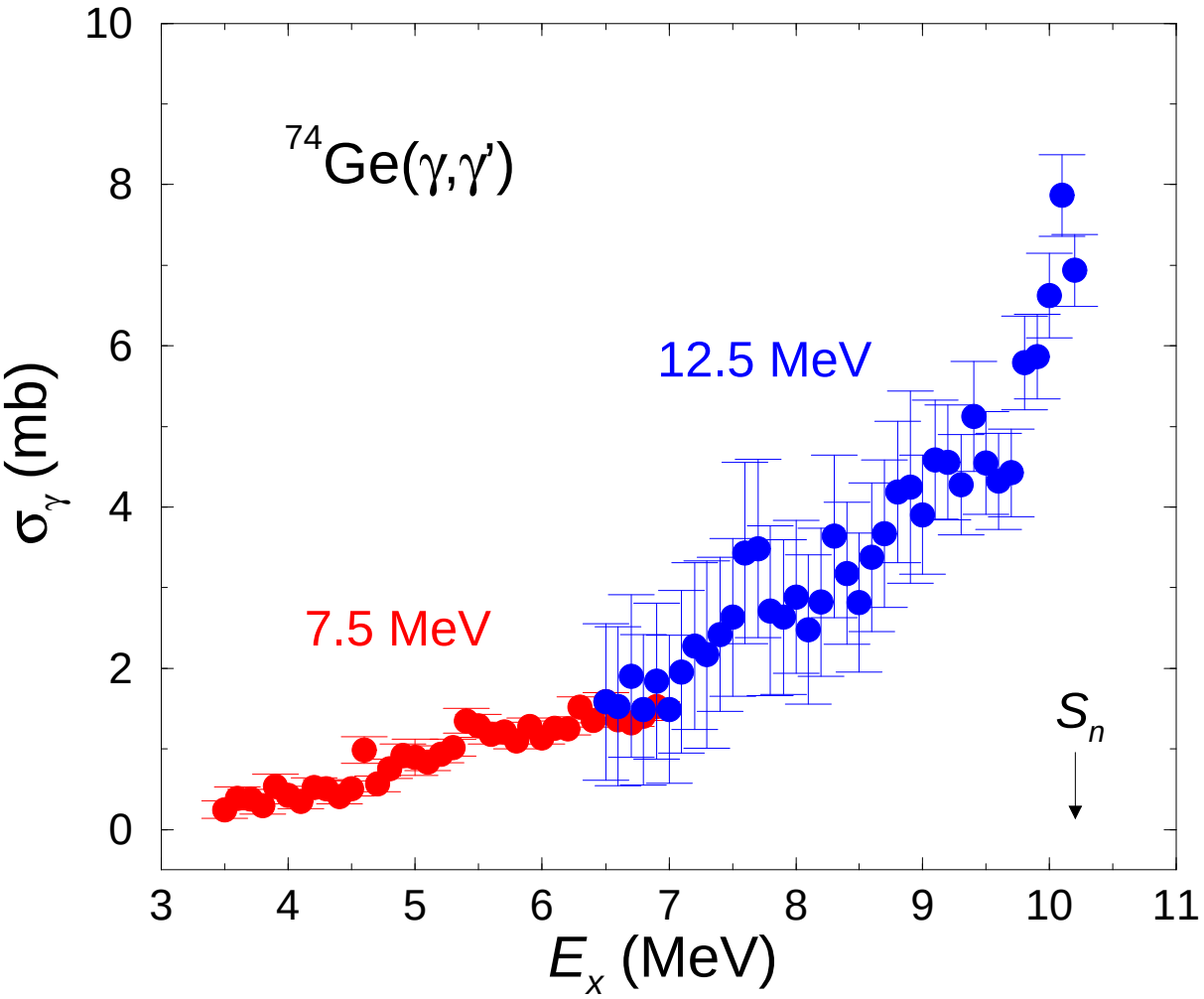

Absorption cross section of ^{74}Ge

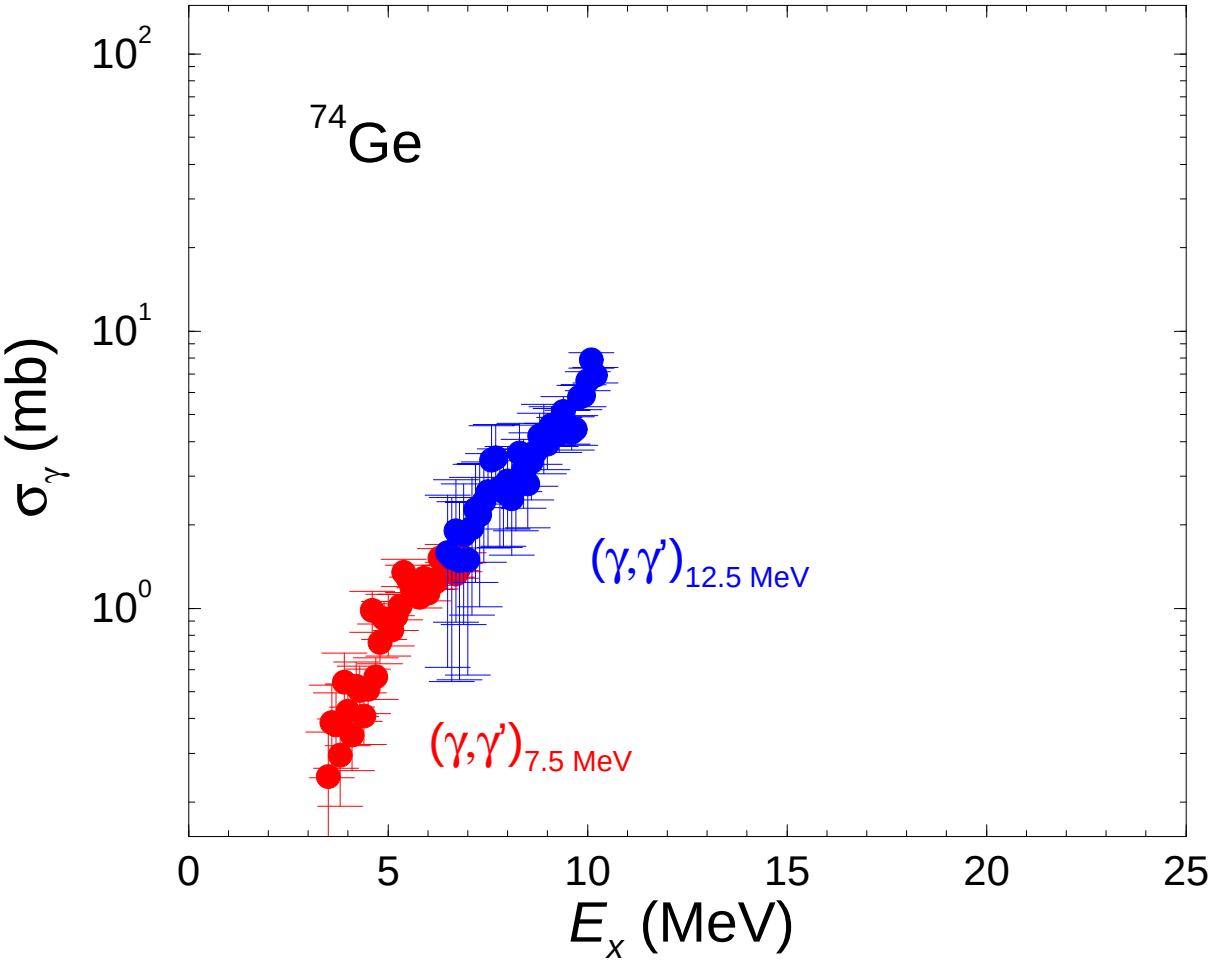

Absorption cross section of ^{74}Ge

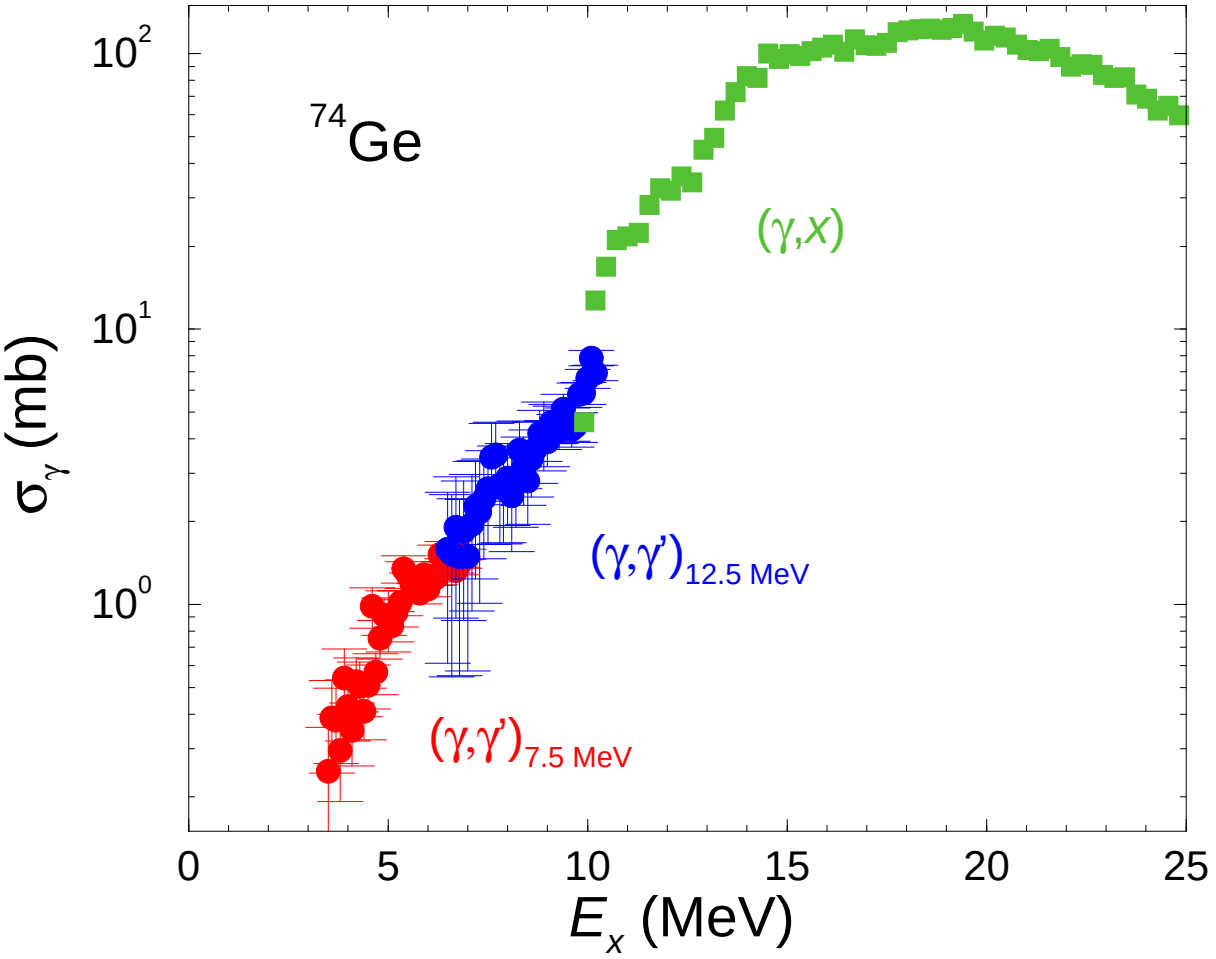

(γ,x) data:

P. Carlos et al.,

NPA 258, 365 (1976)

Absorption cross section of ^{74}Ge

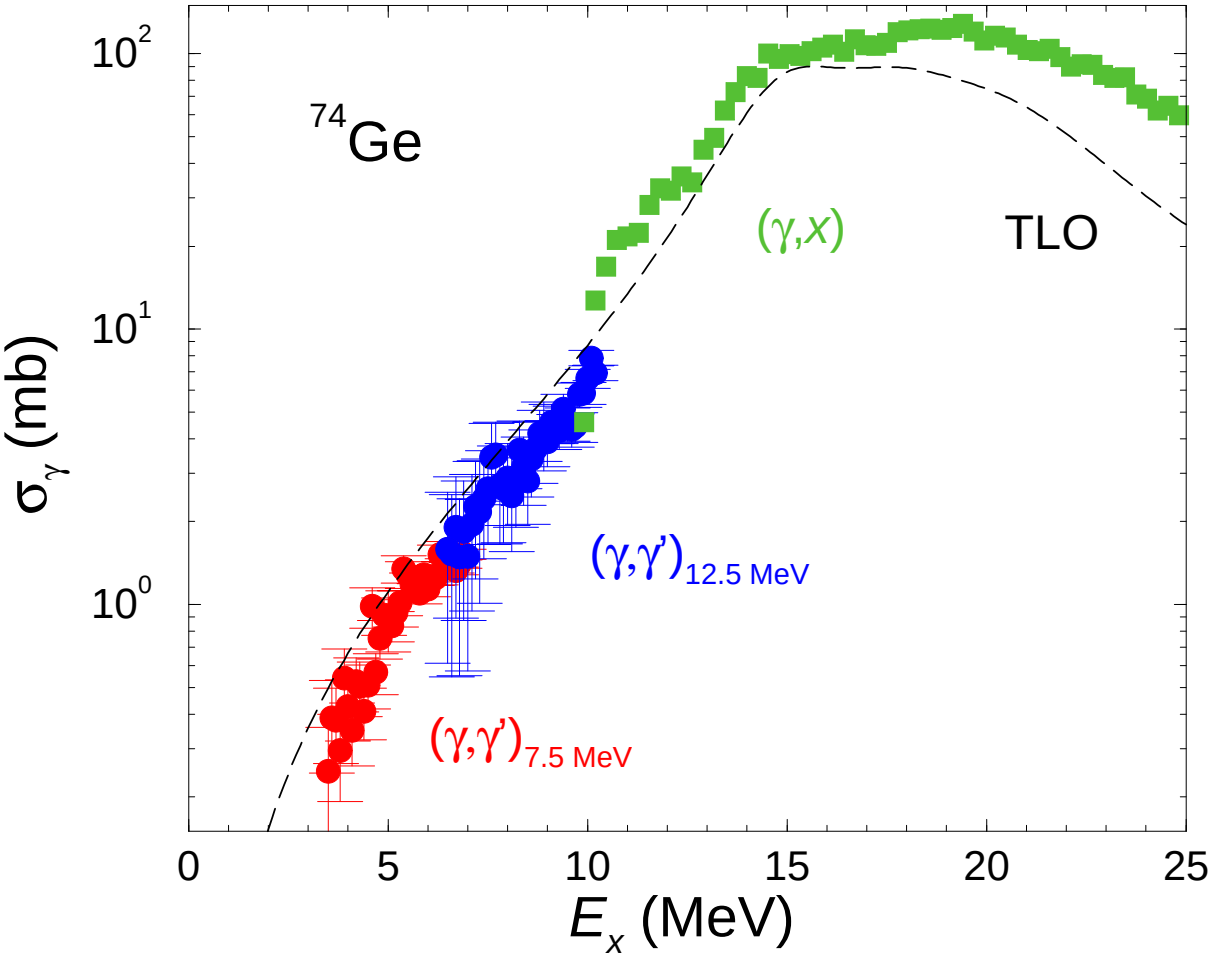

(γ,x) data:

P. Carlos et al.,

NPA 258, 365 (1976)

TLO ($\beta_2 = 0.28$, $\gamma = 27°$):

A. Junghans et al.,

PLB 670, 200 (2008)

Electromagnetic strength functions

- Electromagnetic strength functions (photon strength functions) describe average electromagnetic transitions strengths - in particular in the quasi-continuum of nuclear states at high excitation energy:

$$f_{fiL}(E_\gamma) = \overline{\Gamma_{fiL}}\ \rho(E_i, J_i)\ /\ E_\gamma^{2L+1} \qquad E_\gamma = E_i - E_f \qquad J_i = 0,\ ...,\ J_{\max}$$

- Photoabsorption:

$$f_L = \sigma_\gamma\ /\ [(2J_i{+}1)/(2J_0{+}1)\ (\pi\hbar c)^2\ E_\gamma^{2L-1}] \qquad E_\gamma = E_i \qquad J_i = 1,\ (2)$$

- Brink-Axel hypothesis:
  The strength function does not depend on the excitation energy.
  The strength function for excitation is identical with the one for deexcitation.

Dipole strength functions in ^{74}Ge

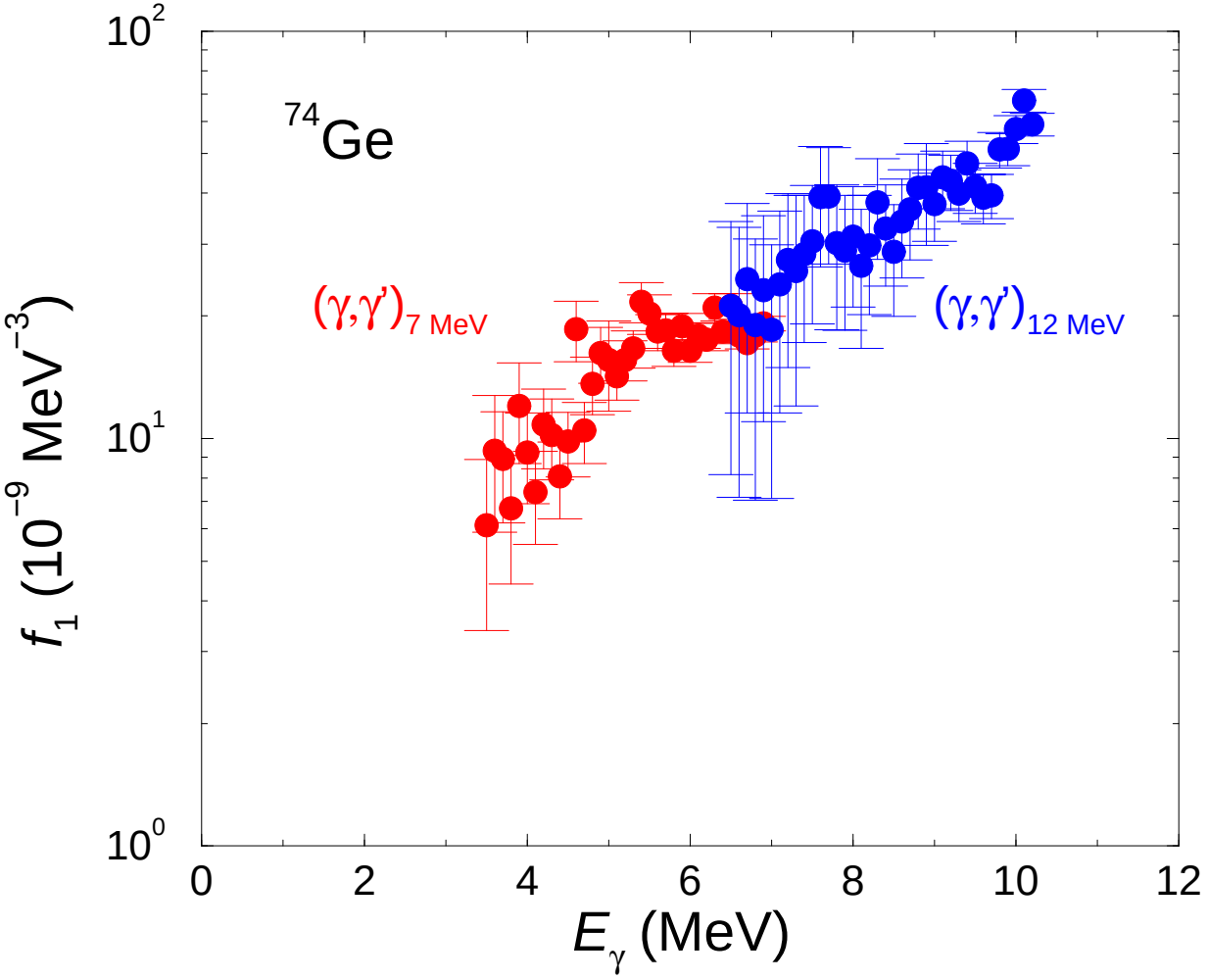

Dipole strength functions in ^{74}Ge

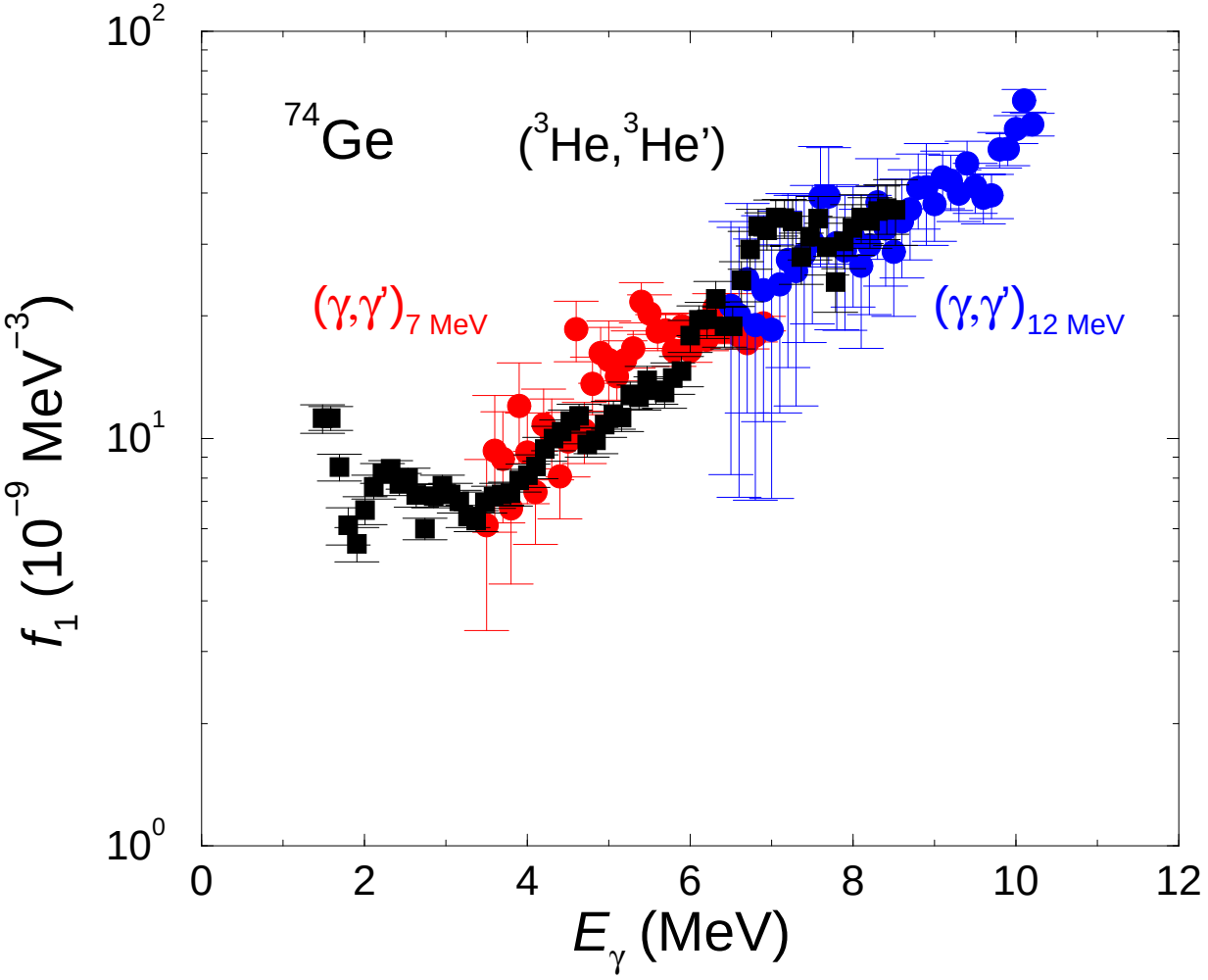

(^{3}He,^{3}He') data:

T. Renstrøm et al.

Dipole strength functions in ^{74}Ge

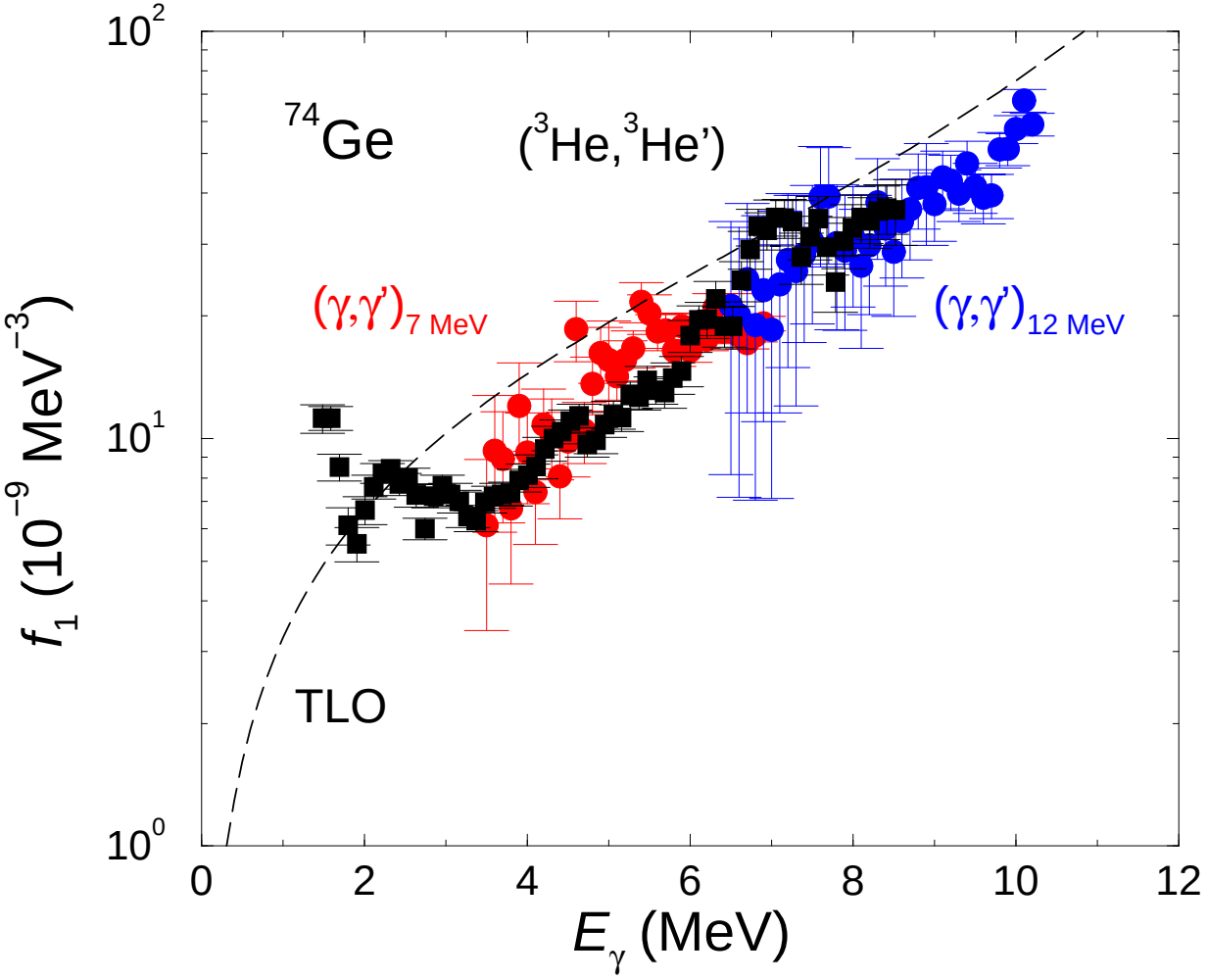

(^{3}He,^{3}He') data:

T. Renstrøm et al.

Dipole strength functions in ^{74}Ge

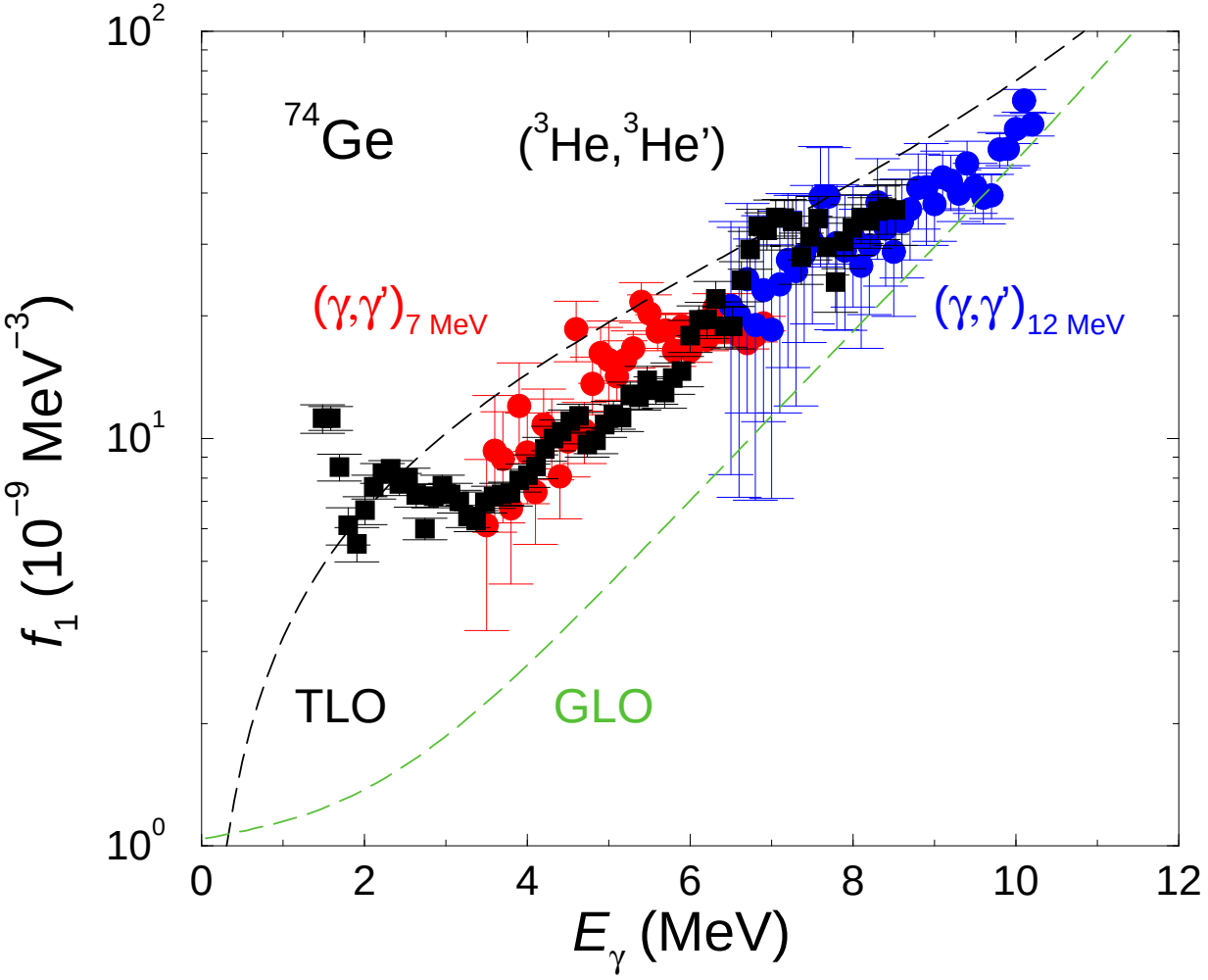

(^{3}He,^{3}He') data:

T. Renstrøm et al.

Shell-model calculations of M1 strength functions

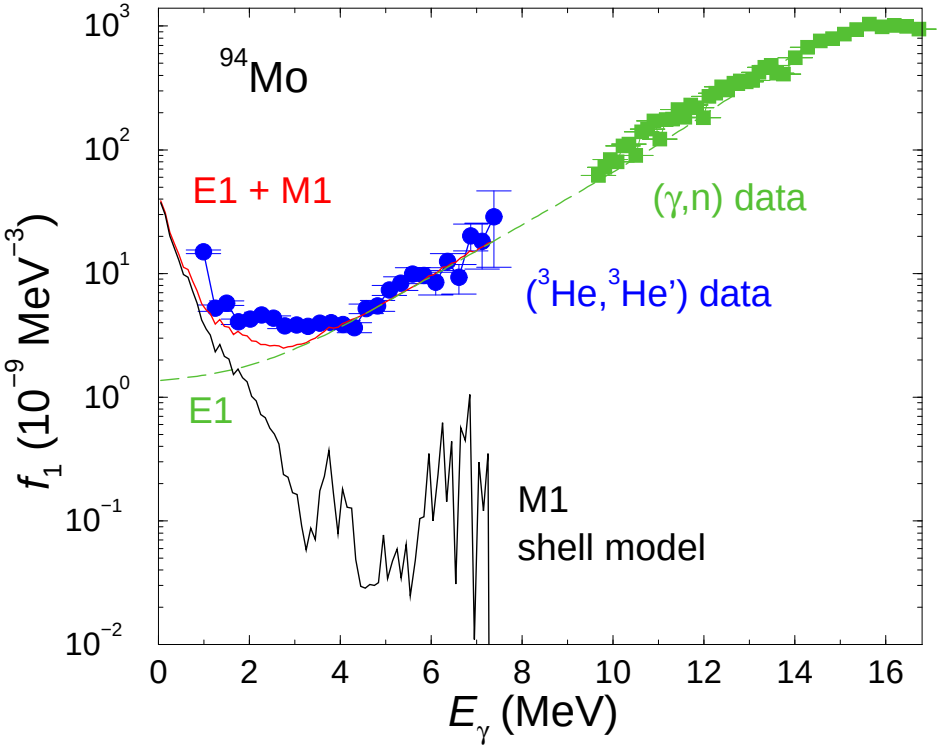

RITSSCHIL

R.S., S. Frauendorf, A.C. Larsen
PRL 111, 232504 (2013)

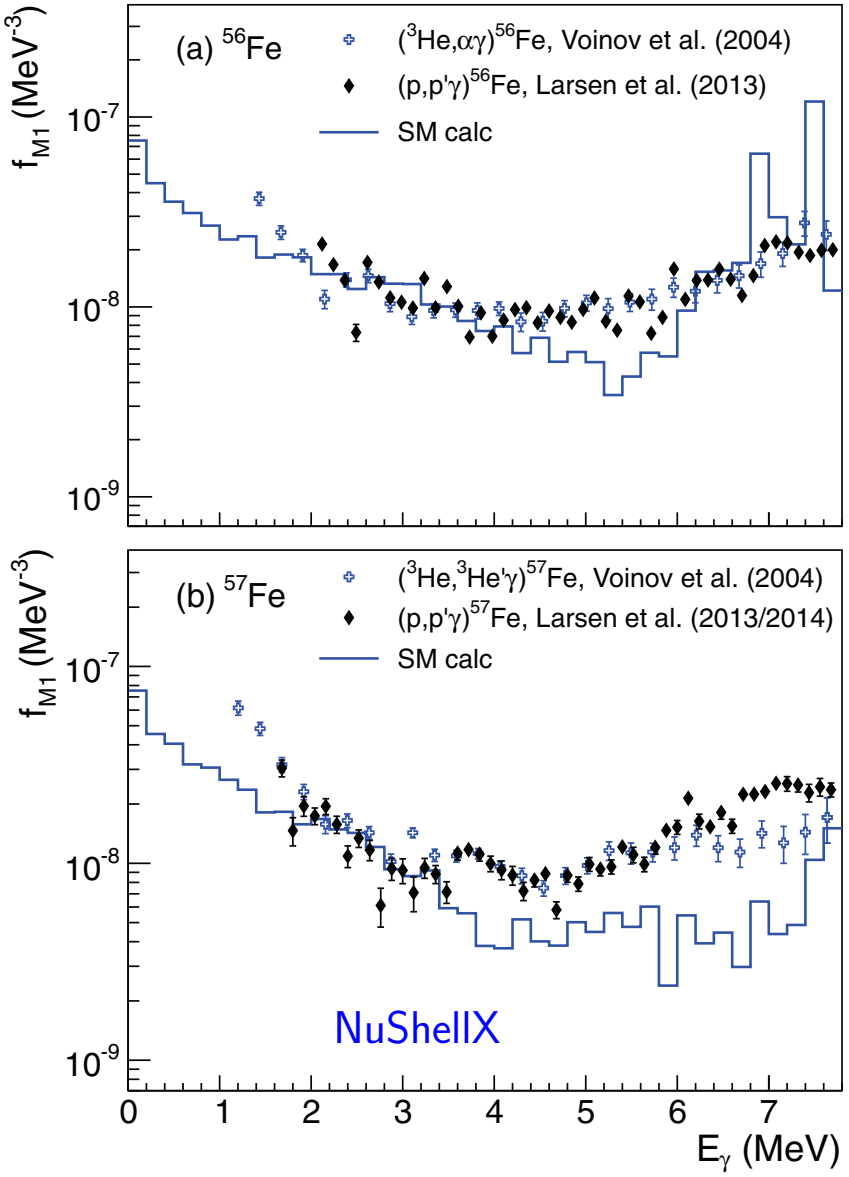

NuShellX

B.A. Brown, A.C. Larsen
PRL 113, 252502 (2014)

Generation of large M1 strengths

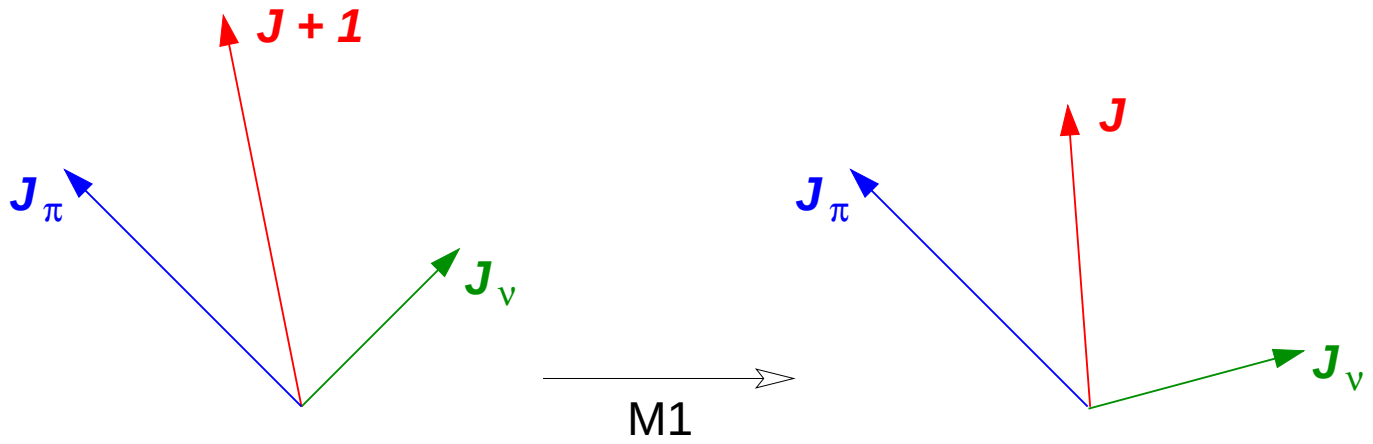

⇒ Configurations including protons *and* neutrons in specific high-j orbits with large magnetic moments.

⇒ Coherent superposition of proton and neutron contributions for specific combinations of g_π and g_ν factors and relative phases ("mixed symmetry").

⇒ Large M1 strengths appear between states with equal configurations by a recoupling of the proton and neutron spins (analog to the "shears mechanism").

Dipole strength functions in ^{74}Ge

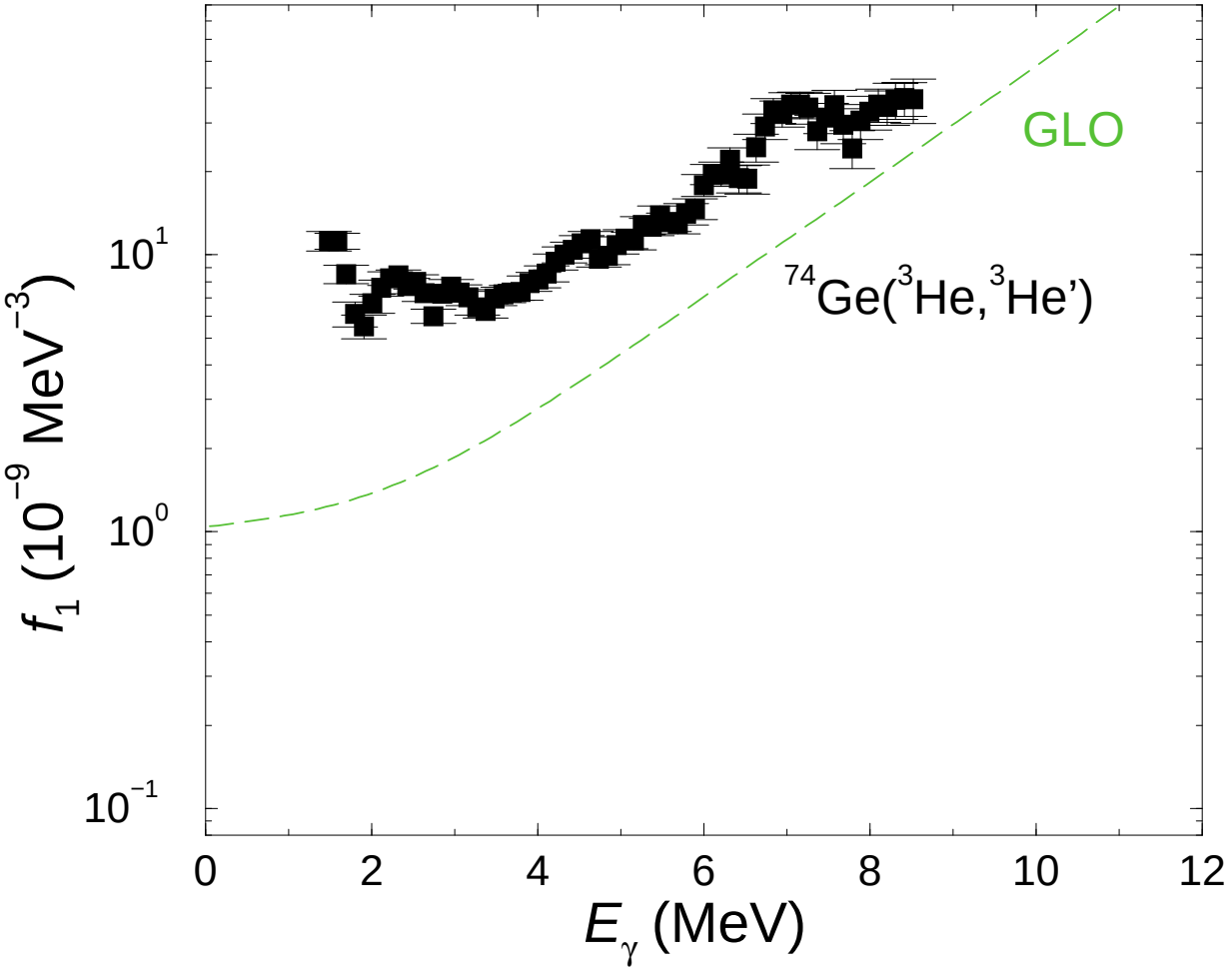

(^{3}He,^{3}He') data:

T. Renstrøm et al.

Dipole strength functions in ^{74}Ge

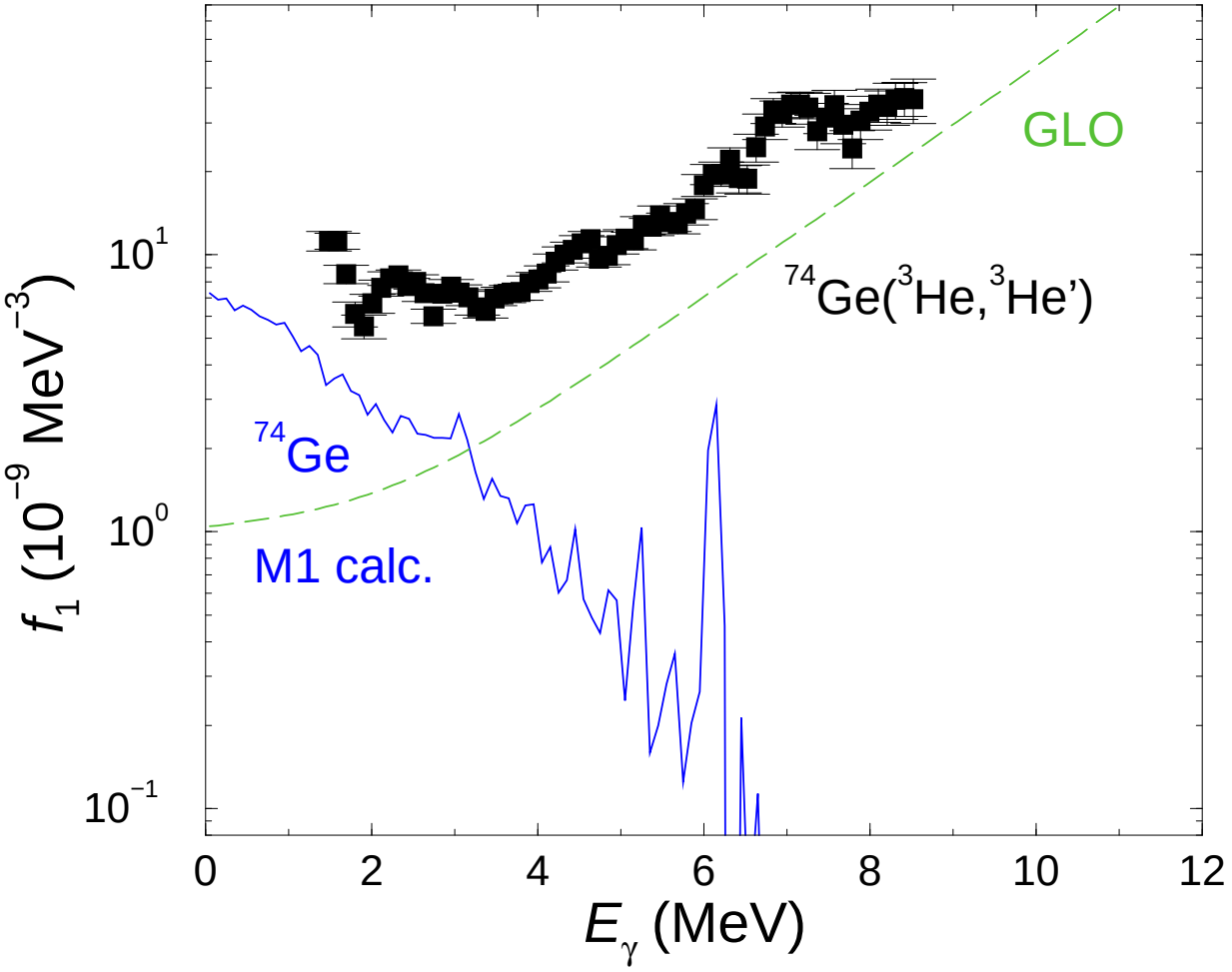

(^{3}He,^{3}He') data:

T. Renstrøm et al.

RITSSCHIL

Dipole strength functions in ^{74}Ge

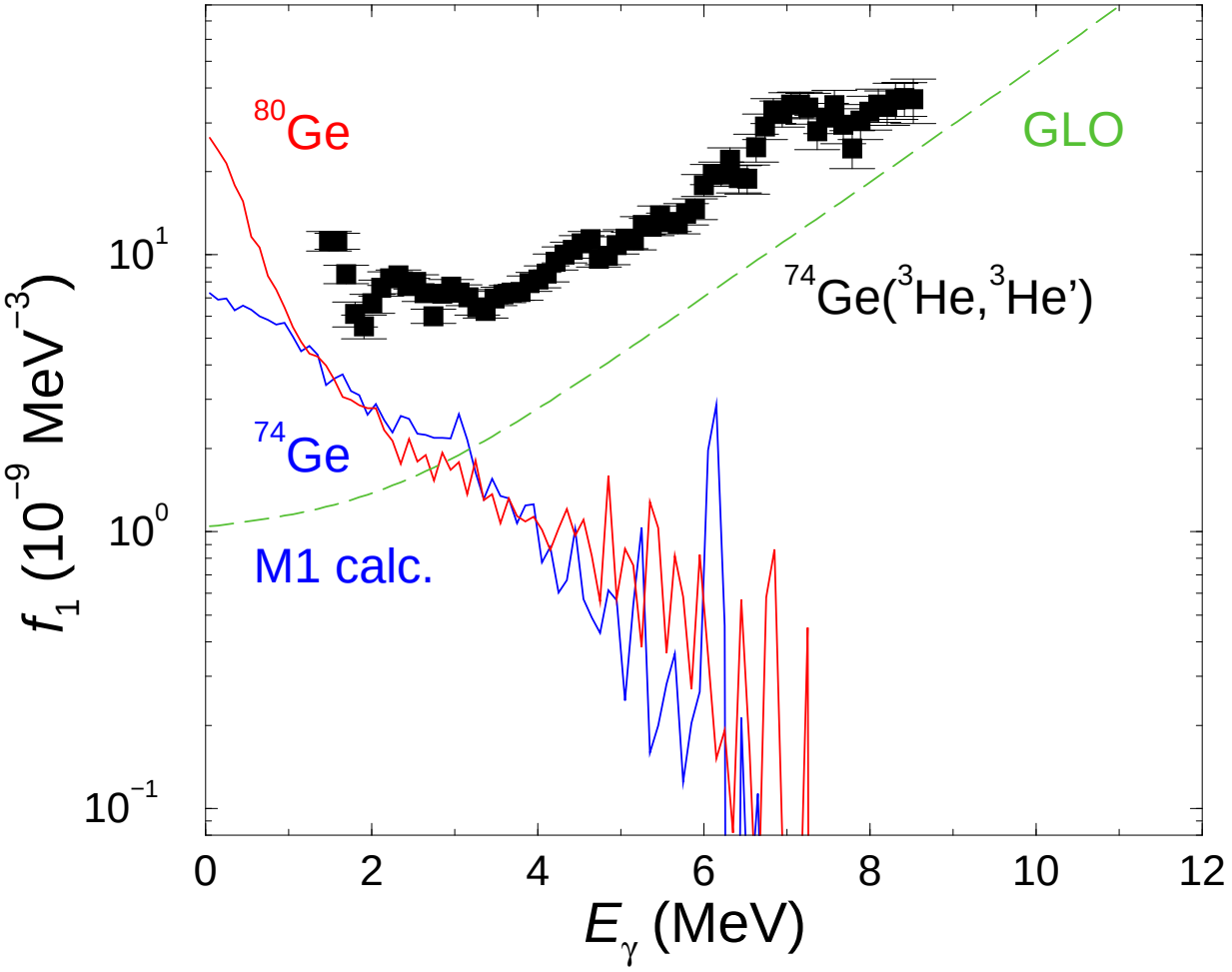

RITSSCHIL

(^{3}He,^{3}He') data:

T. Renstrøm et al.

Predicted Appearance of magnetic rotation

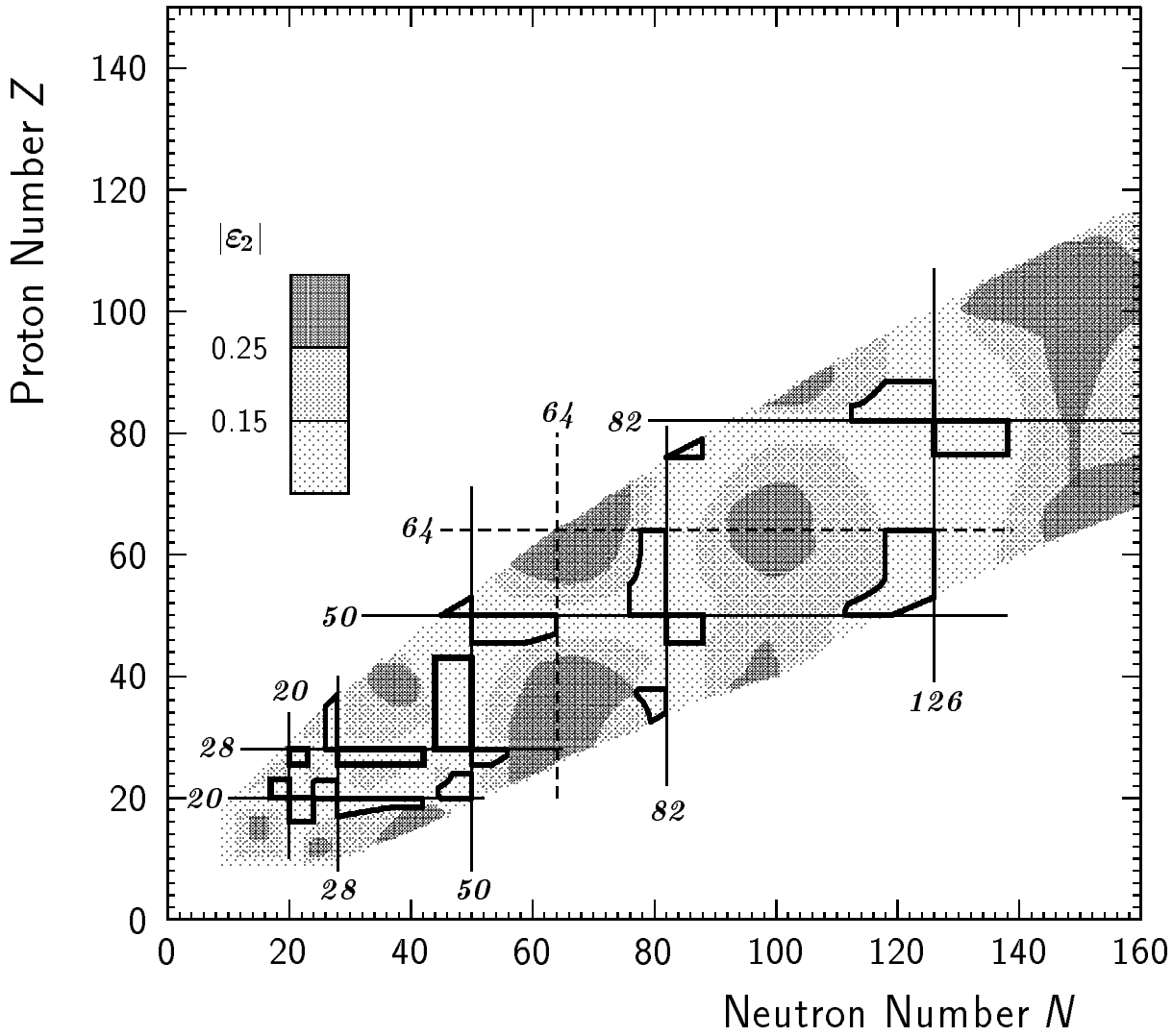

S. Frauendorf, Rev. Mod. Phys. 73, 463 (2001).

Generation of large M1 strengths

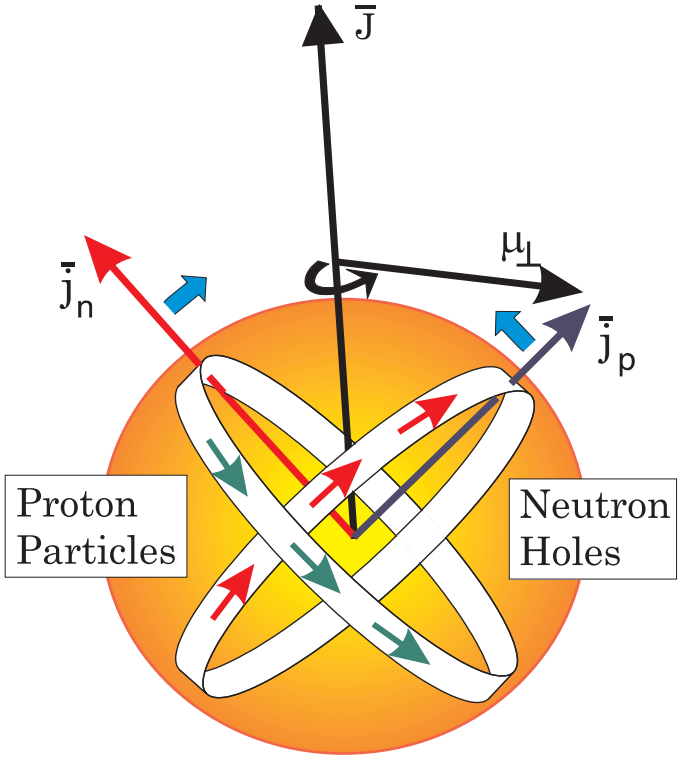

$B(\mathrm{M1}) \sim \mu_\perp^2$

Analogous “shears mechanism”
in magnetic rotation

S. Frauendorf, Rev. Mod. Phys. 73, 463 (2001).

Examples near $A = 80$: ^{82}Rb, ^{84}Rb

H. Schnare et al., PRL 82, 4408 (1999).

R.S. et al., PRC 66, 024310 (2002).

Shell-model calculations for ^{74}Ge and ^{80}Ge

Main configurations that generate large M1 transition strengths (active orbits with $j_\pi \neq 0$ and $j_\nu \neq 0$):

^{74}Ge	$\pi = +$:	$\pi(0f_{5/2}^4)$	$\nu(0g_{9/2}^2)$	$\pi = -$:	$\pi(0f_{5/2}^4)$	$\nu(1p_{1/2}^{-1}\ 0g_{9/2}^3)$
		$\pi(0f_{5/2}^3\ 1p_{3/2}^1)$	$\nu(0g_{9/2}^2)$		$\pi(0f_{5/2}^3\ 1p_{3/2}^1)$	$\nu(1p_{1/2}^{-1}\ 0g_{9/2}^3)$
		$\pi(0f_{5/2}^2\ 1p_{3/2}^2)$	$\nu(0g_{9/2}^2)$		$\pi(0f_{5/2}^2\ 1p_{3/2}^2)$	$\nu(1p_{1/2}^{-1}\ 0g_{9/2}^3)$
^{80}Ge	$\pi = +$:	$\pi(0f_{5/2}^4)$	$\nu(0g_{9/2}^8)$	$\pi = -$:	$\pi(0f_{5/2}^3\ 0g_{9/2}^1)$	$\nu(0g_{9/2}^8)$
		$\pi(0f_{5/2}^3\ 1p_{3/2}^1)$	$\nu(0g_{9/2}^8)$		$\pi(0f_{5/2}^2\ 1p_{3/2}^1\ 0g_{9/2}^1)$	$\nu(0g_{9/2}^8)$
		$\pi(0f_{5/2}^3\ 1p_{3/2}^1)$	$\nu(0g_{9/2}^7\ 1d_{5/2}^1)$		$\pi(0f_{5/2}^3\ 0g_{9/2}^1)$	$\nu(0g_{9/2}^7\ 1d_{5/2}^1)$

$\Rightarrow$ Configurations including a broken $\nu 0g_{9/2}$ pair in addition to π(fp) excitations.

E2 strength function in ^{94}Mo

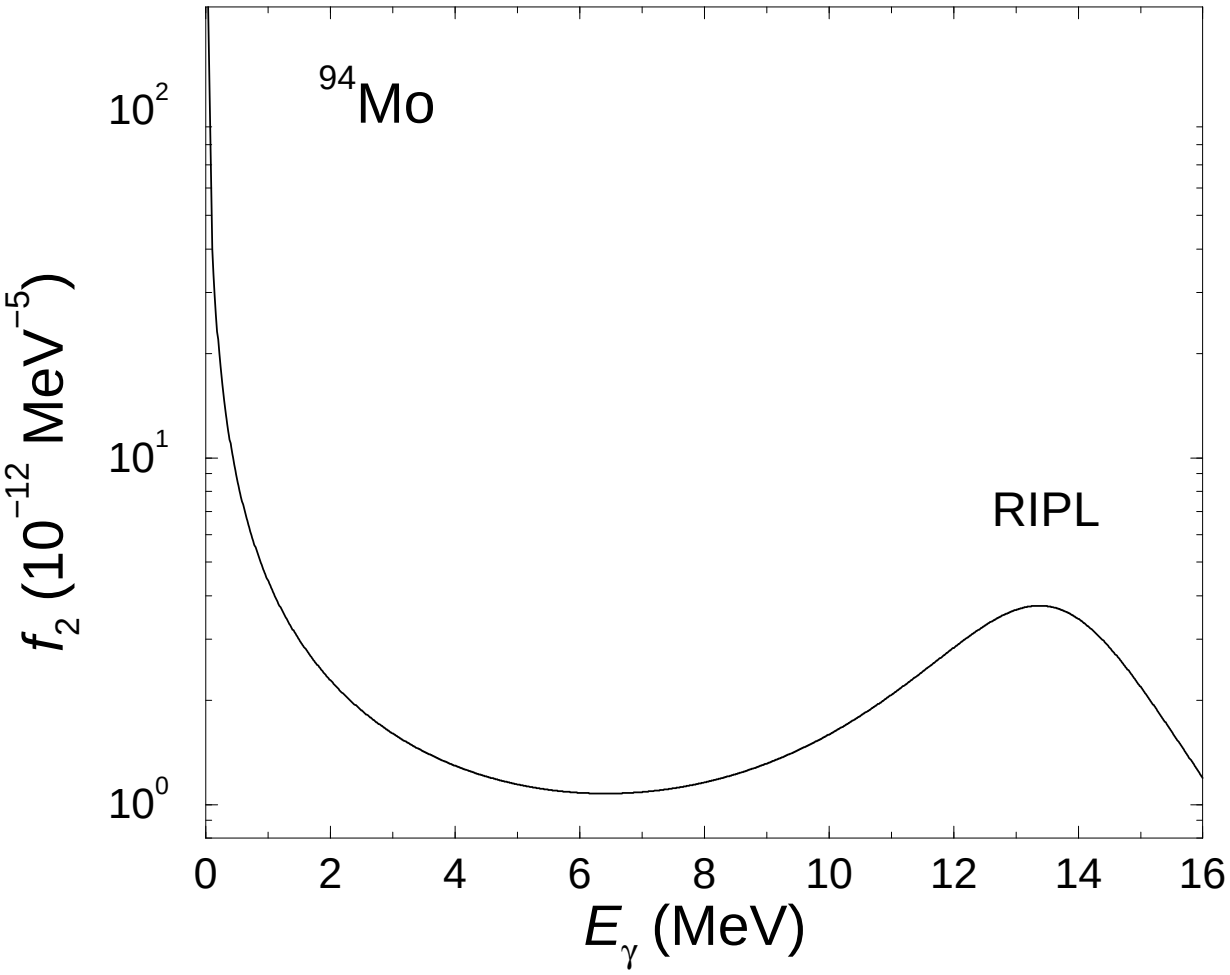

E2 strength function in RIPL

Lorentz curve with:

$E_{max} = 63\ A^{-1/3}$ MeV

$\Gamma = 6.11 - 0.021A$ MeV

$\sigma_{\gamma,max} = 0.00014\ Z^2 E_{max} A^{-1/3} \Gamma^{-1}$ mb

R.S., PRC 90, 064321 (2014)

E2 strength function in ^{94}Mo

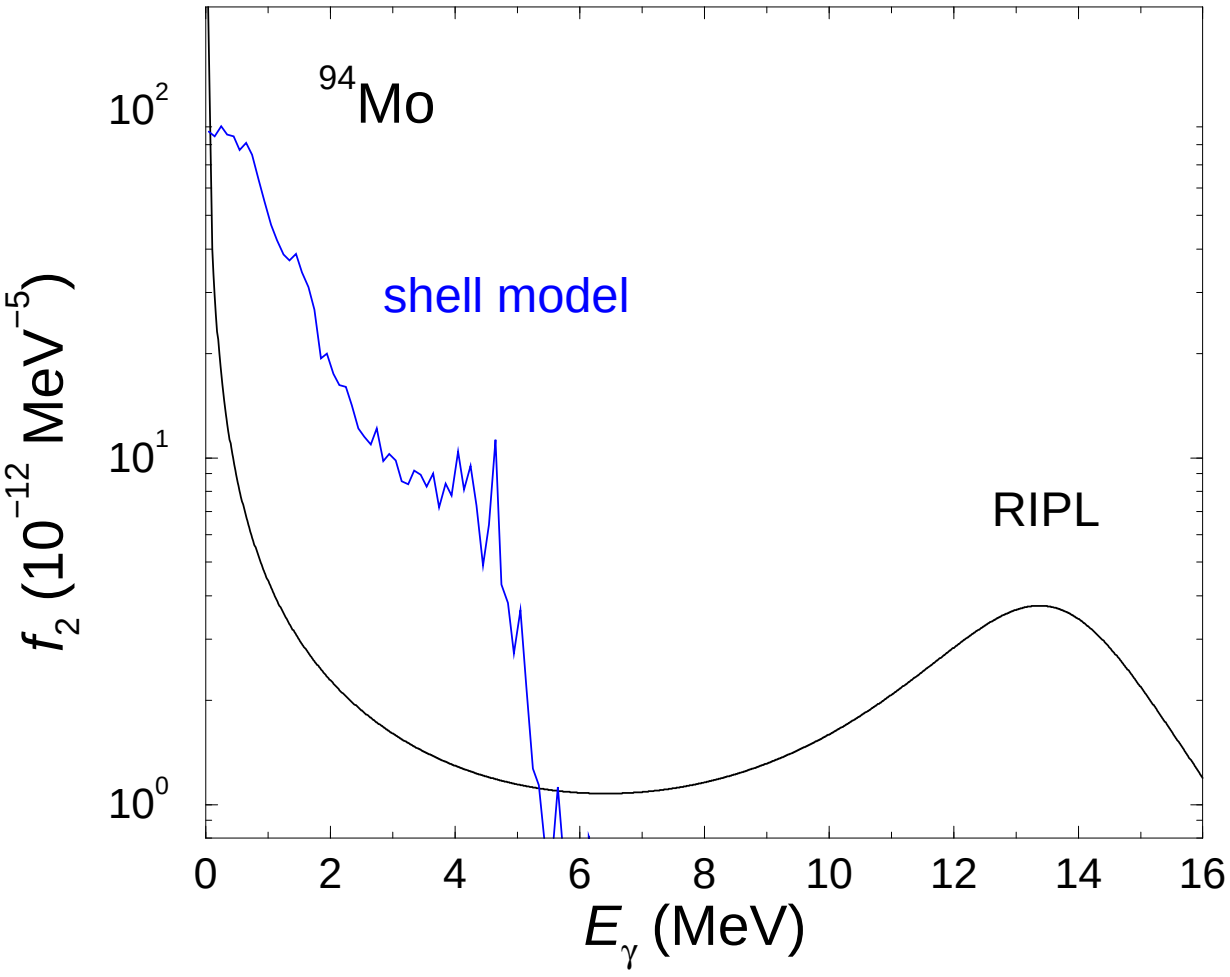

RITSSCHIL

E2 strength function

$f_2 = 0.80632\ \overline{B(\mathrm{E2})}\ \rho(E_{x,J})$

$\rho(E_x, J)$ - level density

of the shell-model states,

includes $\pi = \pm 1$,

$J = 0$ to 10,

40 states for each J^π.

R.S., PRC 90, 064321 (2014)

E2 strength function in ^{94}Mo

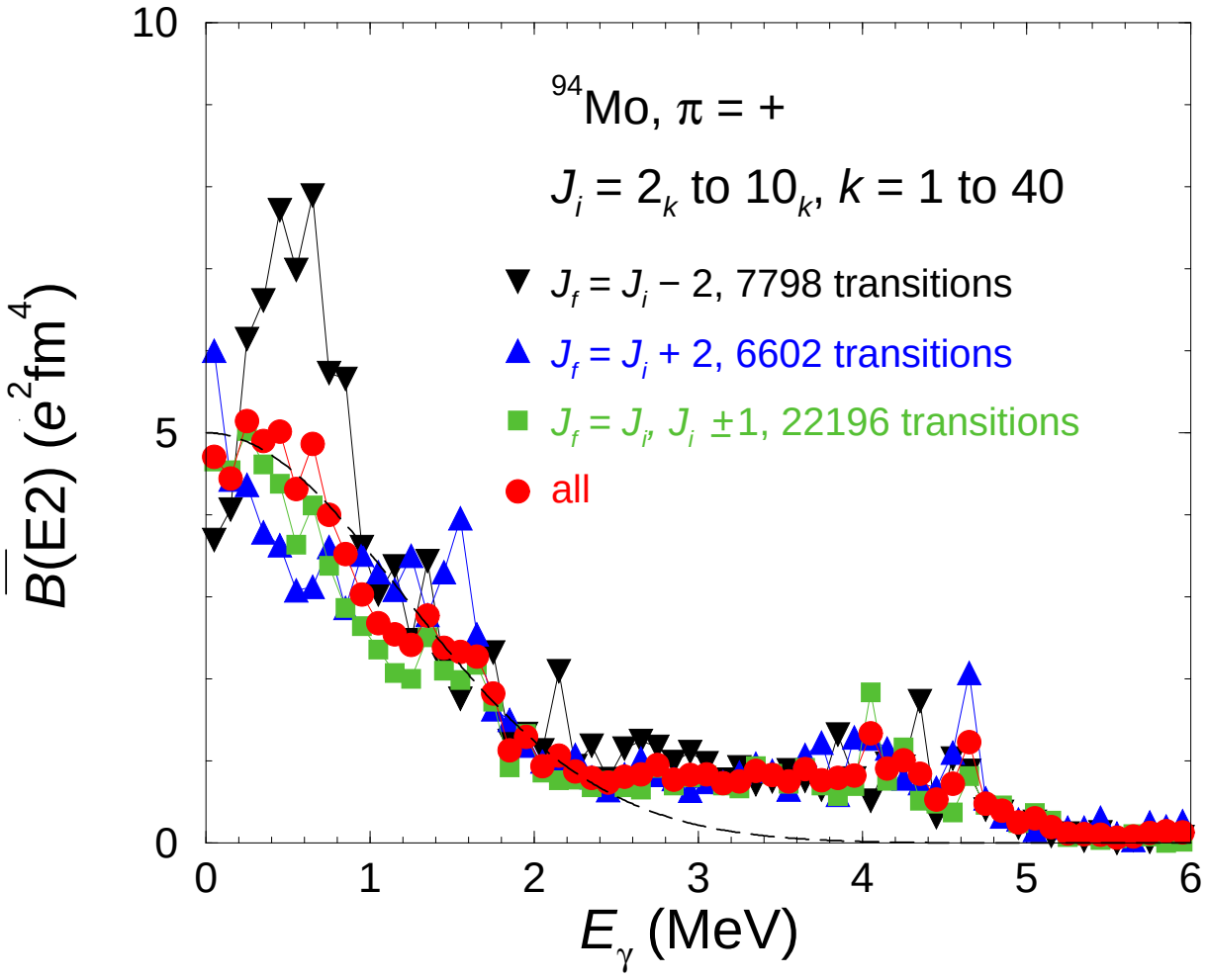

RITSSCHIL

R.S., PRC 90, 064321 (2014)

E2 strength function in ^{74}Ge

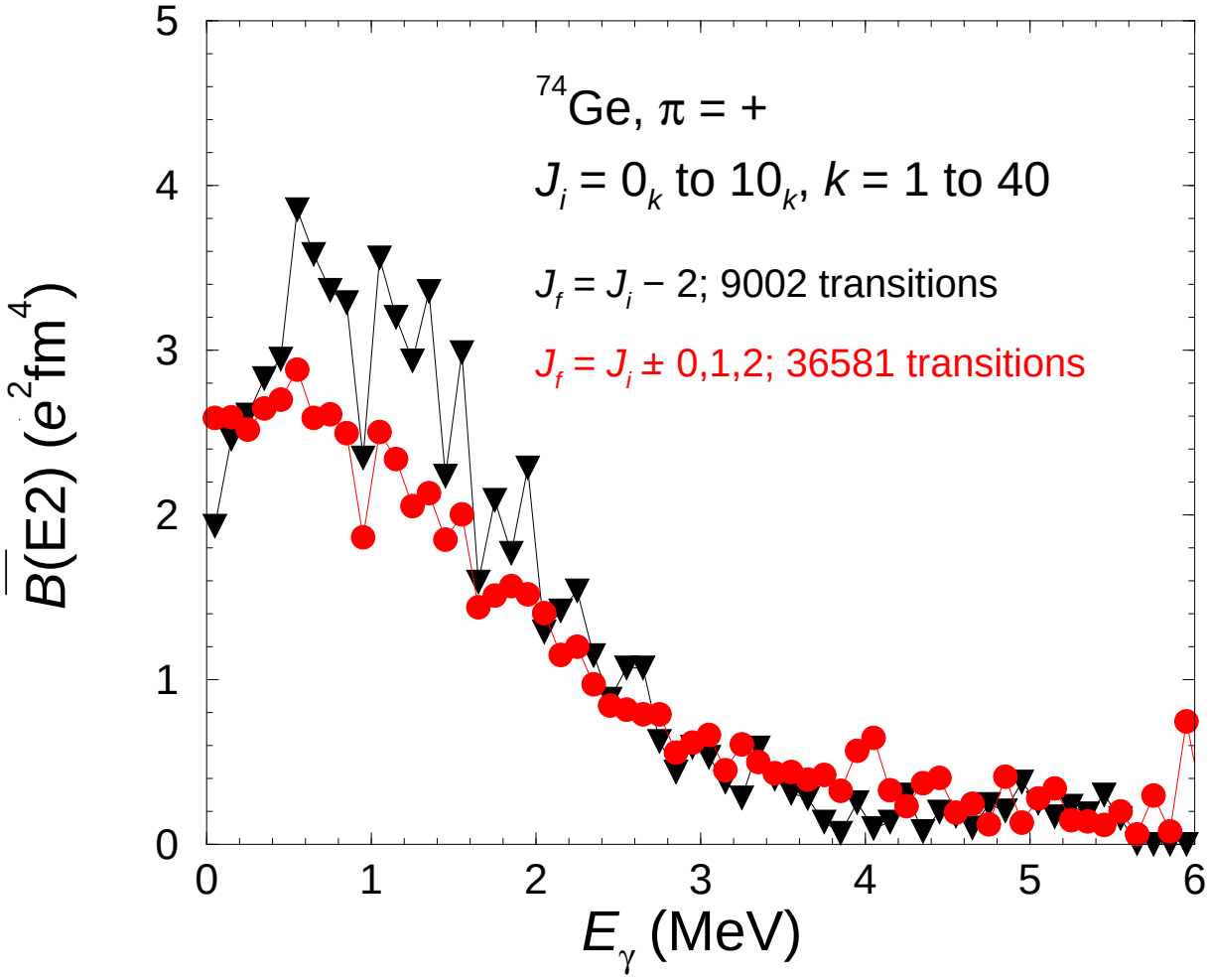

RITSSCHIL

E2 strength function in ^{64}Fe

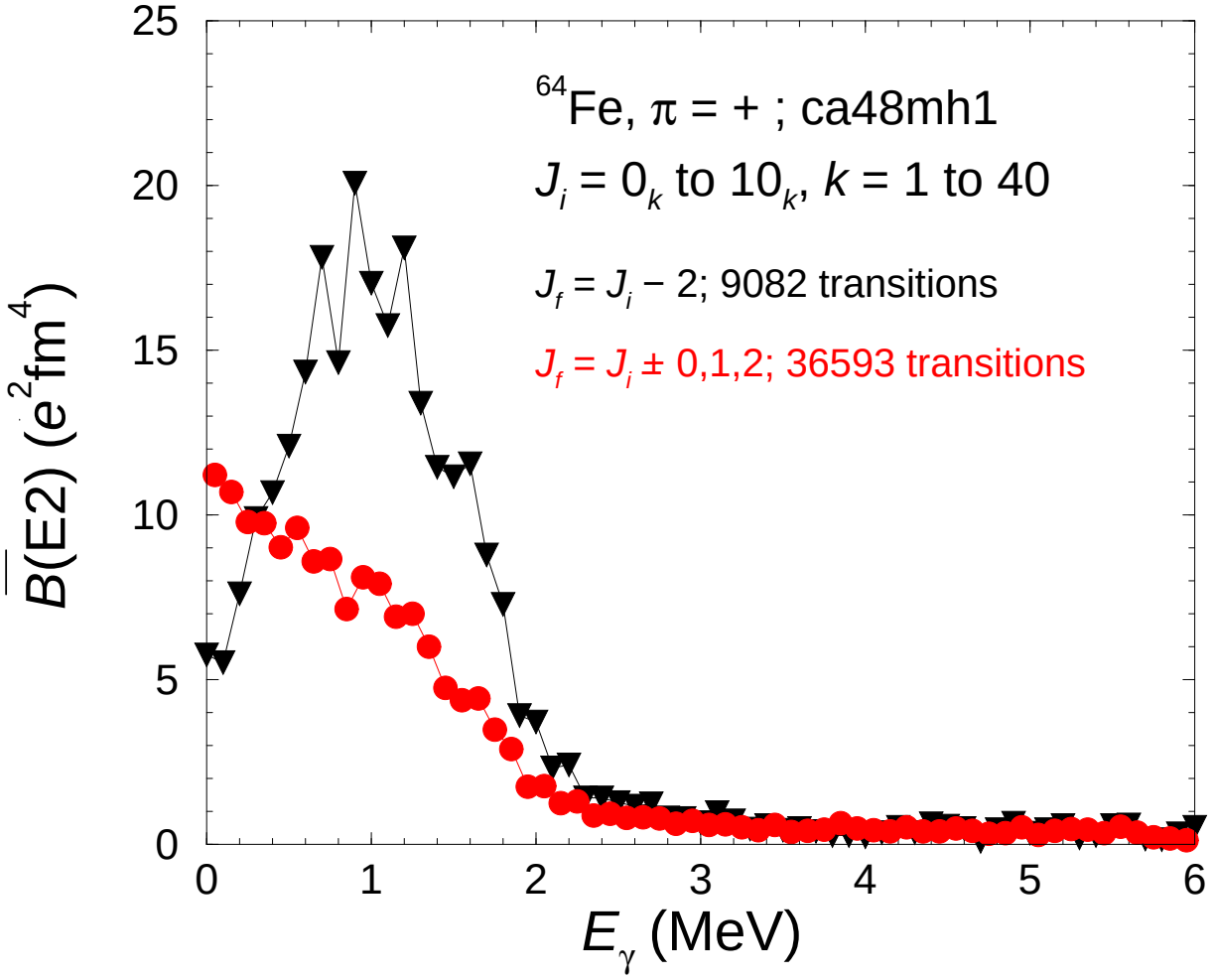

$B(\mathrm{E2}, 2_1^+ \rightarrow 0_1^+)_{\mathrm{exp}} = 470^{+210}_{-110}$ e^2fm^4

J. Ljungvall et al., PRC 81, 061301 (2010)

$B(\mathrm{E2}, 2_1^+ \rightarrow 0_1^+)_{\mathrm{calc}} = 406$ e^2fm^4

NuShellX: B.A. Brown, W.D.M. Rae, NDS 120, 115 (2010)

Summary

- Photon-scattering experiments on ^{74}Ge with bremsstrahlung at γELBE using 7.5 and 12.1 MeV electrons.
- Determination of the dipole strength function at high excitation energy and high level density. Inclusion of strength in the quasicontinuum and correction of the observed strength for branching and feeding by using statistical methods.
- No considerable enhancement of E1 strength in the pygmy region.
- Good agreement between the strength functions deduced from the present (γ, γ') experiments and from (^{3}He,^{3}He') experiments.
- Low-energy enhancement observed in the (^{3}He,^{3}He') experiment qualitatively described by M1 strength functions calculated within the shell model.
  Large M1 strengths result from a recoupling of the spins of specific high-j proton and neutron orbits.
- E2 strength functions at low energy calculated within the shell model show similar characteristics in various mass regions and are at variance with approximations recommended in RIPL.

Collaborators

Motivation:	L.A. Bernstein (LLNL, Univ. Berkeley)
Data analysis:	R. Massarczyk (HZDR, LANL)
Data acquisition:	A. Wagner
Technical assistence:	A. Hartmann
Experimenters:	M. Anders, D. Bemmerer, R. Beyer, Z. Elekes, R. Hannaske, A.R. Junghans, T. Kögler, M. Röder, K. Schmidt, L. Wagner